Universal Speed Limit in a Far-from-Equilibrium Bose Gas: Symmetry and Dynamical Decoherence

Jun-Cheng Liang[1,*] and Bo Chen[2]

[1] *Department of Physics, Weinan Normal University, Weinan 714099, China*
[2] *School of Physics and Optoelectronic Engineering, Beijing University of Technology, Beijing 100124, China*

(Dated: May 13, 2026)

Predicting universal transport coefficients in far-from-equilibrium quantum systems remains a fundamental challenge. A paradigmatic example is the non-thermal fixed point (NTFP) of isolated Bose gases, where coherence spreads as $\ell^2(t) = C\hbar t/m$ with a universal constant C. While the scaling exponent $z = 2$ is well established, the amplitude C has remained elusive because the underlying particle cascade $n(k) \sim k^{-4}$ leads to a divergent kinetic energy, threatening the very existence of a constant speed limit. Here we resolve this paradox and present the first analytical, parameter-free prediction of a universal amplitude C. A deep interplay between symmetry and dissipation is uncovered. The emergent weak U(1) symmetry at the NTFP enforces a conserved total current, forcing the low-energy phase dynamics to obey a diffusive Langevin equation with noise entering as the divergence of a stochastic current. This structure, combined with dynamical decoherence of high-momentum modes, yields a universal power-law momentum distribution $\tilde{f}(v) \sim (1 + v^2)^{-3}$ (with $v = k\ell$) that naturally regularizes the ultraviolet divergence. From this, a parameter-free geometric baseline $C = 3$ is obtained, independent of microscopic details. The experimental value $C = 3.4(3)$ [Martirosyan et al., Nature 647, 608 (2025)] is then shown to be quantitatively consistent with universal logarithmic corrections arising from a marginally irrelevant coupling at the fixed point. A new paradigm is thus established for predicting transport coefficients in strongly correlated non-equilibrium systems: symmetry constraints determine the low-energy effective theory, dynamical decoherence provides a natural ultraviolet completion, and scaling analysis delivers testable predictions moving beyond scaling exponents to quantitative amplitude prediction.

Keywords: Universal Speed Limit, Non-thermal Fixed Point, Weak U(1) Symmetry, Dynamical Decoherence

I. INTRODUCTION

Universal dynamics in far-from-equilibrium quantum many-body systems represent a frontier across physics, from the early universe [1] and quark-gluon plasmas [2] to quantum many-body systems [3–12]. Such dynamics are often bounded by fundamental limits, from the speed of light to the Lieb-Robinson bound for information propagation [13]. A unifying concept in this context is that of non-thermal fixed points (NTFPs) [14–17], which act as attractors in the renormalization group (RG) flow of isolated systems far from equilibrium [18–20]. Earlier experiments have revealed universal scaling dynamics across dimensions: the $z = 2$ fixed point has been observed in two-dimensional Bose gases [21], where vortex clustering can give rise to an anomalously slow scaling exponent [22], and in spinor systems [23, 24], as well as in three-dimensional homogeneous [25] and trapped [26] gases. Quasi-one-dimensional systems exhibit a distinct scaling exponent $\beta \approx 0.1$ in the weakly interacting regime [27]; strong interactions induce a crossover toward $\beta \approx 0.5$, suggestive of the $z = 2$ fixed point [28]. For a comprehensive overview of NTFP experiments in Bose gases, we refer to the recent reviews [29, 30]. A profound recent example emerges in isolated Bose gases, where coarsening dynamics collapse onto a $z = 2$ fixed point ($\beta = 1/2$) with a universal speed limit: $d\ell^2/dt = C\hbar/m$ and $C = 3.4(3)$, a rate set solely by the quantum of velocity circulation and remarkably robust against variations in initial conditions, interaction strength, and density [31]. This experimental observation point toward the existence of fundamental constraints on the speed of coherence propagation, representing a distinct type of speed limit beyond the Lieb-Robinson bound [32].

Analogous to equilibrium critical phenomena [33], the NTFP framework synthesizes and extends earlier theoretical approaches such as Bose condensation kinetics [34–36] and wave turbulence theory [37, 38]. Key foundations for the present work include non-perturbative kinetic theory, which established the cascade spectrum $n(k) \sim k^{-4}$ and the universal infrared scaling of the effective coupling $g_{\rm eff}(p) \sim p^2$ in the collective-scattering regime [17]; earlier field-theoretic studies that identified the self-similar scaling properties of the NTFP [16]; low-energy effective theories that revealed the symmetry structure of the phase dynamics [30, 39]; and hydrodynamic descriptions that connect scaling to transport [40]. While these efforts successfully predicted the universal scaling exponent $z = 2$, a prediction later confirmed experimentally [31], the associated transport coefficient C remained inaccessible because the formally divergent kinetic energy integral arising from the k^{-4} cascade renders its direct evaluation cutoff dependent. Resolving this paradox requires a physical

mechanism that naturally tames high-momentum contributions while preserving the symmetry constraints that govern low-energy dynamics.

Despite decades of progress, the non-thermal fixed point (NTFP) of Bose gases has yielded only the scaling exponent $z = 2$; the universal transport coefficient C has remained inaccessible due to an ultraviolet divergence paradox. Recent developments in gauge-invariant response theory for Lindbladian open systems have shown that weak U(1) symmetry, rather than strict particle-number conservation, is the essential requirement for current conservation in dissipative settings [41]. Although our system is isolated, the dynamical decoherence of high-momentum modes effectively mimics an open-system environment for the low-energy phase dynamics. This emergent openness, combined with the spontaneous breaking of U(1) symmetry at the NTFP, endows the system with an effective weak U(1) symmetry in the sense of Ref. [41]. Here we resolve this paradox and present the first analytical prediction of the universal amplitude C. It is first proven that emergent weak U(1) symmetry governs diffusive dynamics ($z = 2$) at the NTFP via modified Ward identities, establishing the fundamental relation $C = 4mD_\phi^{\rm macro}/\hbar$. The crucial insight is that high-momentum modes, although populated in the cascade, rapidly lose phase coherence and decouple from collective transport. This dynamical decoherence provides a physical ultraviolet completion, in stark contrast to the ad-hoc cutoffs or fitting parameters used in earlier numerical simulations (see, e.g., Refs. [17, 30]). From this, a parameter-free geometric baseline is obtained: $C = 3$: an exact rational number, not a fitted parameter. This number arises not from fitting but from the geometric structure of the power-law momentum distribution $\tilde{f}(v) \sim (1 + v^2)^{-3}$ (or equivalently v^{-6}), replacing the divergent integral of the bare cascade. This baseline corresponds to the idealized fixed point with infinite scale separation. For finite scale separation $\ell/\xi \sim 50$ as realized experimentally, universal logarithmic corrections arise from a marginally irrelevant coupling, yielding $C = 3.4(3)$ in agreement with measurement [31]. A new paradigm is thus established for predicting transport coefficients in strongly correlated non-equilibrium systems: symmetry constraints determine the low-energy effective theory, dynamical decoherence provides a natural ultraviolet completion, and scaling analysis delivers testable predictions that go beyond scaling exponents to quantitative amplitude prediction. This paradigm parallels equilibrium critical phenomena, but here the weak U(1) symmetry and decoherence-driven UV cutoff are intrinsically dynamical. The power-law momentum distribution emerges as a generic regulator, suggesting that this mechanism may be broadly operative across far-from-equilibrium systems. Together with recent advances in universal speed limits on quantum scrambling [12], fermionic quantum criticality [42], and gauge-invariant response theory [41], the present results indicate that symmetry-protected universality and decoherence-driven UV regularization are generic features of far-from-equilibrium quantum matter.

II. GROSS-PITAEVSKII DESCRIPTION AND EMERGENT SCALING

The universal dynamics observed in the experiment [31] occur in a regime where the dilute Bose gas is well described by the Gross-Pitaevskii equation (GPE). For a three-dimensional homogeneous system at ultra-low temperature $T \ll T_c$, with weak interactions $na^3 \ll 1$, the macroscopic wave function $\psi(\mathbf{r}, t)$ evolves according to

$$i\hbar\frac{\partial\psi}{\partial t} = -\frac{\hbar^2}{2m}\nabla^2\psi + g|\psi|^2\psi, \tag{1}$$

where $g = 4\pi\hbar^2 a/m$ is the interaction strength determined by the s-wave scattering length a [43, 44]. The healing length $\xi = \hbar/\sqrt{2mgn}$ sets the microscopic scale below which density variations become important. Equation (1) is justified under the experimental conditions of Ref. [31]: (i) ultra-low temperature $T \ll T_c$; (ii) weak interactions $na^3 \ll 1$; (iii) dynamics dominated by long wavelengths ($\ell(t) \gg \xi$), where $\ell(t)$ is the growing coherence length. Via the Madelung transformation $\psi = \sqrt{n}e^{i\phi}$, the GPE correctly captures the evolution of the macroscopic phase field ϕ that governs coherence propagation. Crucially, near a NTFP the universal behavior is independent of microscopic details; the GPE, embodying the essential U(1) symmetry and conservation laws, therefore correctly determines the universality class [14].

Emergent scale invariance at the NTFP is revealed by considering the GPE under the dynamic scaling transformation

$$\mathbf{x} \to \lambda\mathbf{x}, \quad t \to \lambda^z t, \quad \psi \to \lambda^{-\alpha}\psi. \tag{2}$$

Under this transformation the terms of Eq. (1) scale as

$$i\hbar\partial_t\psi \sim \lambda^{-z-\alpha}, \tag{3}$$

$$-\frac{\hbar^2}{2m}\nabla^2\psi \sim \lambda^{-2-\alpha}, \tag{4}$$

$$g|\psi|^2\psi \sim \lambda^{-3\alpha}. \tag{5}$$

Form invariance of the GPE requires all terms to scale identically, yielding the conditions

$$-z - \alpha = -2 - \alpha = -3\alpha, \tag{6}$$

which uniquely determine the exponents

$$\alpha = 1, \qquad z = 2. \tag{7}$$

The value $z = 2$ implies diffusive growth of the coherence length, $\ell(t) \sim t^{1/2}$, consistent with both kinetic theory [17] and experimental observations [31].

It is important to emphasize that while the GPE correctly identifies the universality class (i.e., the exponent $z = 2$), it cannot predict the universal amplitude C appearing in $d\ell^2/dt = C\hbar/m$. The reason is twofold. First, as a deterministic, reversible, and conservative equation, the GPE lacks any dissipation or noise; it therefore cannot capture the dynamical decoherence of high-momentum modes that naturally cuts off the ultraviolet divergence of the bare cascade $n(k) \sim k^{-4}$. Second, although the GPE respects U(1) symmetry and yields the correct low-energy diffusive pole $\chi_{\phi\phi} = (-i\omega + D_\phi k^2)^{-1}$, it does not determine the numerical value of the phase diffusion coefficient D_ϕ because the latter depends on the strength of the effective noise and on the detailed ultraviolet shape of the momentum distribution. Consequently, the amplitude C is governed by the specific form of the scaling function and its ultraviolet regularization, which require the field-theoretic framework developed in the following sections.

III. SYMMETRY-CONSTRAINED DIFFUSIVE DYNAMICS AT THE NTFP

Having established the GPE description and scaling analysis, we now develop the symmetry-constrained framework that governs the diffusive dynamics at the NTFP. Starting from the Keldysh field theory, we derive the modified Ward identity arising from the strong U(1) transformation. Combined with the dynamic scaling exponent $z = 2$, this identity forces the phase response to take the diffusive form $\chi_{\phi\phi}(k,\omega) = (-i\omega + D_\phi k^2)^{-1}$. We then relate the microscopic phase diffusion coefficient D_ϕ to a macroscopic, scale-independent coefficient $D_\phi^{\rm macro}$, and finally connect the latter to the universal constant C via $C = 4mD_\phi^{\rm macro}/\hbar$. This section thus constructs a hierarchical framework from microscopic symmetry to macroscopic effective field theory, providing the basis for the quantitative evaluation of C in Sec. IV.

A. Keldysh field theory and modified Ward identity

We employ the Keldysh closed-time path integral formalism, the fundamental framework for non-equilibrium quantum many-body systems [6, 45–48]. The microscopic action in the Keldysh basis is

$$S[\psi_c,\psi_q] = \int dt d^3x \Big[\psi_q^*\left(i\hbar\partial_t + \frac{\hbar^2}{2m}\nabla^2\right)\psi_c + \text{c.c.} - \frac{g}{2}|\psi_c|^2(\psi_c^*\psi_q + \psi_q^*\psi_c) + i\hbar\gamma\left(\psi_q^*\psi_c + \psi_c^*\psi_q\right) + i\hbar\tilde{D}|\psi_q|^2\Big], \tag{8}$$

where ψ_c and ψ_q denote the classical and quantum fields, respectively. The parameters γ and $\tilde{D}$ represent effective dissipation and noise arising from integrating out fast modes in the many-body scattering processes that lead to the NTFP [17]. Although the dissipative terms explicitly break U(1) symmetry at the microscopic level, at the NTFP the system exhibits an emergent approximate symmetry that constrains the long-wavelength dynamics.

The consequences of this approximate symmetry are encoded in modified Ward identities. To derive them, we employ the *strong U(1) transformation* (opposite phase rotations on the forward and backward Keldysh contours):

$$\psi_+(x) \to e^{i\theta(x)}\psi_+(x), \qquad \psi_-(x) \to e^{-i\theta(x)}\psi_-(x), \tag{9}$$

which in the Keldysh basis becomes

$$\begin{aligned} &\delta\psi_c = i\theta\psi_q, \quad \delta\psi_q = i\theta\psi_c, \\ &\delta\psi_c^* = -i\theta\psi_q^*, \quad \delta\psi_q^* = -i\theta\psi_c^*. \end{aligned} \tag{10}$$

This transformation is a technical tool; it is not a symmetry of the dissipative action, but its variation yields exact identities that incorporate dissipation.

The total action splits into a conserved part $S_{\rm cons}$ (kinetic and interaction terms) and a dissipative part $S_{\rm diss}$ (the last two terms in Eq. (8)). Under the strong U(1) transformation, the variation of $S_{\rm cons}$ gives the divergence of the Noether current:

$$\delta S_{\rm cons} = \int_x \theta(x)\big[-\partial_t j^0(x) + \nabla\cdot\mathbf{j}(x)\big] + \mathcal{O}(\theta^2), \tag{11}$$

with density and current $j^0 = \hbar|\psi_c|^2$ and $\mathbf{j} = \frac{\hbar^2}{2mi}(\psi_c^*\nabla\psi_c - \psi_c\nabla\psi_c^*)$. The variation of $S_{\rm diss}$ is obtained by direct functional differentiation:

$$\delta S_{\rm diss} = -\hbar(\gamma+\tilde{D})\int_x \theta(x)\big(\psi_q^*\psi_c - \psi_c^*\psi_q\big). \tag{12}$$

Invariance of the path integral measure under the transformation leads to an exact Ward identity. Following the standard Keldysh procedure (see Appendix A2 for details), we introduce linear response sources, take functional derivatives, and Fourier transform. The resulting exact identity, before any fixed-point simplification, reads

$$\omega\chi_{n\phi}(k,\omega) - \frac{\hbar n_0}{m}k^2\chi_{\phi\phi}(k,\omega) = 2i(\gamma+\tilde{D})\,\chi_{\rm mix}(k,\omega) + \Delta_{\rm quantum}, \tag{13}$$

where $n_0 = \langle|\psi_c|^2\rangle$ is the average density, $\chi_{n\phi}$ and $\chi_{\phi\phi}$ are the retarded density-phase and phase-phase response functions, and $\chi_{\rm mix}$ denotes the retarded response of the composite operator $\psi_q^*\psi_c - \psi_c^*\psi_q$ (up to a constant factor). The term $\Delta_{\rm quantum}$ collects higher-order quantum correlations, which are negligible in the classical-wave

regime ($n_k \gg 1$) characteristic of the NTFP. This condition defines the regime where the GPE applies and quantum statistics are suppressed, so that Δ_{quantum} can be safely dropped.

At the NTFP, two simplifications occur. First, the low-energy dynamics is governed by the phase fluctuations; both the density fluctuation and the operator $\psi_q^*\psi_c - \psi_c^*\psi_q$ couple linearly to the phase field in the long-wavelength limit. Consequently, their response functions share the same scaling form, implying a constant ratio

$$\chi_{\text{mix}}(k,\omega) = \beta_0\, \chi_{n\phi}(k,\omega) \qquad (k \to 0,\ \omega/k^2 \text{ fixed}), \tag{14}$$

with a universal dimensionless constant β_0. Second, scale invariance at the $z = 2$ fixed point fixes the ratio of noise to dissipation coefficients to a universal constant,

$$\frac{\tilde{D}}{\gamma} = \alpha_0, \tag{15}$$

where α_0 is also universal (see Appendix A2 for its origin from an emergent fluctuation-dissipation-like relation).

Substituting Eqs. (14) and (15) into the exact identity (13) and dropping the quantum term Δ_{quantum} yields

$$\omega\chi_{n\phi} - \frac{\hbar n_0}{m}k^2\chi_{\phi\phi} = 2i\gamma(1+\alpha_0)\beta_0\,\chi_{n\phi}. \tag{16}$$

It is natural to combine the fixed-point constants into a single effective dissipation coefficient

$$\gamma_{\text{eff}} \equiv \gamma(1+\alpha_0)\beta_0, \tag{17}$$

which is a universal constant at the NTFP. The modified Ward identity then takes the compact form

$$\omega\chi_{n\phi}(k,\omega) - \frac{\hbar n_0}{m}k^2\chi_{\phi\phi}(k,\omega) = 2i\gamma_{\text{eff}}\chi_{n\phi}(k,\omega), \tag{18}$$

where the superscript R (retarded) is omitted for simplicity. The right-hand side explicitly reflects the presence of dissipation and distinguishes this identity from its equilibrium counterpart.

The strong U(1) transformation is a technical tool whose variation yields the exact identities that incorporate dissipation. The physical system itself, however, possesses an exact *weak U(1) symmetry* (identical phase rotations on both contours), which guarantees the conservation of the total current and provides the microscopic foundation for the noise construction employed later (see Appendix A3). As shown in the general weak-U(1) Ward-Takahashi identity of Ref. [41], the total current (kinetic plus dissipative) is conserved, $\partial_\mu J_c^\mu = 0$. Equation (18) is the low-energy manifestation of that general identity for our system, with the term $2i\gamma_{\text{eff}}\chi_{n\phi}$ representing the dissipative part of the current, the key symmetry constraint that determines the structure of the phase response at the fixed point.

B. Emergent diffusive dynamics from scaling and symmetry

Dimensionless convention. In this subsection all quantities (k, ω, χ, γ_{eff}) are understood to be dimensionless; they have been rescaled by appropriate powers of the healing length ξ and the time scale $\tau_0 = m\xi^2/\hbar$. Constants such as $\hbar n_0/m$ that appear in the equations are implicitly absorbed into the definitions of the scaling functions $\Phi(u)$ and $\Psi(u)$; their explicit retention is only for notational consistency with the original Ward identity. This convention simplifies the algebra and highlights the universal scaling properties.

At the NTFP, the system exhibits emergent scale invariance. For a dynamic critical exponent $z = 2$, the phase response function must obey the scaling form

$$\chi_{\phi\phi}(k,\omega) = k^{-2}\Phi(\omega/k^2), \tag{19}$$

where Φ is a universal dimensionless function. Similarly, the density-phase response scales as $\chi_{n\phi}(k,\omega) = k^{-1}\Psi(\omega/k^2)$.

Inserting these scaling ansätze into the modified Ward identity (18) yields

$$uk\Psi(u) - \frac{\hbar n_0}{m}\Phi(u) = 2i\gamma_{\text{eff}}k^{-1}\Psi(u), \qquad u \equiv \omega/k^2. \tag{20}$$

Why a constant γ_{eff} cannot survive. At the $z = 2$ fixed point, the combination $\gamma_{\text{eff}}k^{-2}$ is scale invariant because γ_{eff} has scaling dimension -2 under $\mathbf{x} \to \lambda\mathbf{x}$, $t \to \lambda^2 t$. However, the right-hand side of Eq. (20) contains $2i\gamma_{\text{eff}}k^{-1}$. If γ_{eff} were a constant, this term would diverge as k^{-1} when $k \to 0$, which is incompatible with the left-hand side (where the first term $uk\Psi$ vanishes and the second term is constant). This indicates that a constant γ_{eff} cannot survive at the fixed point; its effect must be absorbed into the renormalized self-energy. Scale invariance alone does not forbid a mass term, but as we now show, the Dyson equation together with the infrared fixed-point structure forces a gapless diffusive mode.

Dyson equation and self-energy expansion. The retarded phase response function satisfies

$$\left[\chi^R_{\phi\phi}(k,\omega)\right]^{-1} = \left[\chi^R_{\phi\phi,0}(k,\omega)\right]^{-1} - \Sigma^R_{\phi\phi}(k,\omega), \tag{21}$$

where $\chi^R_{\phi\phi,0}$ is the free response and $\Sigma^R_{\phi\phi}$ the retarded self-energy. In the Keldysh framework, expanding the action (8) to quadratic order around the condensate and integrating out the quantum field yields the low-energy free inverse response

$$\left[\chi^R_{\phi\phi,0}(k,\omega)\right]^{-1} = -i\omega + \frac{\hbar}{2m}k^2, \tag{22}$$

where the $-i\omega$ term originates from the time derivative (the explicit dissipative term has been absorbed into the self-energy for convenience) and $\frac{\hbar}{2m}k^2$ is the quantum pressure.

At the NTFP, the phase field is the Goldstone mode of the spontaneously broken U(1) symmetry. The Goldstone theorem requires $\Sigma^R_{\phi\phi}(0,0) = 0$. Expanding for small k and ω, spatial rotational invariance and causality (which requires $\mathrm{Re}\,\Sigma^R_{\phi\phi}$ to be even in k and $\mathrm{Im}\,\Sigma^R_{\phi\phi}$ to be odd in ω) dictate the leading terms

$$\Sigma^R_{\phi\phi}(k,\omega) = -i\omega\,\eta_1 + \sigma k^2 + \mathcal{O}(\omega^2, \omega k^2, k^4), \tag{23}$$

with real coefficients $\eta_1 = \partial_\omega \Sigma^R_{\phi\phi}(0,0)$ and $\sigma = \partial_{k^2}\Sigma^R_{\phi\phi}(0,0)$. Substituting (22) and (23) into (21) yields

$$\left[\chi^R_{\phi\phi}\right]^{-1} = -i\omega(1+\eta_1) + \Big(\frac{\hbar}{2m} - \sigma\Big)k^2 + \cdots .$$

From scaling to the diffusive pole. The $z = 2$ scale invariance demands that $\chi_{\phi\phi} \sim k^{-2}\Phi(\omega/k^2)$; therefore the inverse response must scale as k^2 at low energies and, after factoring out the overall scale, can only contain terms linear in ω and k^2 (higher powers would alter the scaling form). The most general low-energy form compatible with analyticity and causality is thus

$$\left[\chi^R_{\phi\phi}\right]^{-1} = Z\,(-i\omega + D_\phi k^2),$$

where Z is a constant (the quasiparticle residue). Identifying coefficients gives $Z = 1+\eta_1$ and $ZD_\phi = \frac{\hbar}{2m} - \sigma$. A nonzero Z can be absorbed by redefining the phase field $\phi \to \phi/\sqrt{Z}$; choosing this normalization such that $Z = 1$ (i.e., $\eta_1 = 0$) is consistent with non-perturbative calculations at the NTFP which show $\partial_\omega \Sigma^R_{\phi\phi}(0,0) = 0$ [17]. With this normalization the inverse response becomes

$$\left[\chi^R_{\phi\phi}(k,\omega)\right]^{-1} = -i\omega + D_\phi k^2, \tag{24}$$

and consequently the full response is

$$\chi_{\phi\phi}(k,\omega) = \frac{-1}{-i\omega + D_\phi k^2}, \tag{25}$$

where D_ϕ is the microscopic phase diffusion coefficient. This diffusive pole is a direct consequence of the combination of emergent scale invariance ($z = 2$), the symmetry constraint embodied in the modified Ward identity, and the infrared scaling of the effective coupling $\Sigma^R_{\phi\phi} \sim k^2$ forced by the non-perturbative fixed-point structure [17]. Such diffusive dynamics has been directly observed in a driven quantum fluid of light near the condensation threshold, where the dynamical critical exponent was found to be $z \approx 2$ [49], and in the vortex imaging experiment of a far-from-equilibrium Bose gas, where the coherence length grows as $\ell^2 \propto t$ and the vortex line-length density decays as $1/t$ [50].

C. Microscopic phase diffusion coefficient and its universal combination

From the expansion (23) we have, at $\omega = 0$,

$$\Sigma^R_{\phi\phi}(0,k) = \sigma k^2 + \mathcal{O}(k^4),$$

and because the imaginary part of the retarded self-energy vanishes at $\omega = 0$ (causality), σ equals the real part

$$\sigma = \lim_{k\to 0} \frac{\mathrm{Re}\,\Sigma^R_{\phi\phi}(0,k)}{k^2}.$$

Using $Z = 1$ and $D_\phi = \frac{\hbar}{2m} - \sigma$ from the previous subsection, we obtain the microscopic expression

$$D_\phi = \frac{\hbar}{2m} - \lim_{k\to 0} \frac{\mathrm{Re}\,\Sigma^R_{\phi\phi}(0,k)}{k^2}, \tag{26}$$

which is the desired relation between the phase diffusion coefficient and the retarded self-energy. The first term $\hbar/(2m)$ originates from the quantum pressure (free diffusion), while the second term subtracts the interaction contribution. The negative sign indicates that interactions effectively reduce the phase stiffness, thereby enhancing D_ϕ compared to the free-particle value.

A key insight from non-perturbative kinetic theory [17] is that at the NTFP the effective many-body coupling exhibits the universal infrared scaling $g_{\mathrm{eff}}(p) \sim p^2$ for momenta p below the healing-length scale $p_\Xi = \sqrt{2mg\rho_{\mathrm{nc}}}$. This scaling suppresses the scattering amplitude at low momenta, ensuring that the imaginary part of the phase self-energy takes the diffusive form $\mathrm{Im}\,\Sigma^R_{\phi\phi}(k,\omega) \sim -D_\phi k^2$ and that the real part $\mathrm{Re}\Sigma^R_{\phi\phi}(0,k)$ is analytic in k^2 with a finite coefficient. Consequently, the limit in (26) is well defined and yields a finite diffusion coefficient.

At the NTFP, scale invariance imposes strong constraints on how D_ϕ depends on the microscopic parameters n and ξ. Because D_ϕ has dimensions of L^2T^{-1} and the only independent scales in the problem are the healing length ξ (length) and the combination $\hbar/m$ (diffusion constant), any dimensionless quantity constructed from D_ϕ, n, and ξ must be a function of the single dimensionless combination $n\xi^3$ (the number of particles in a coherence volume). Hence D_ϕ must take the form

$$D_\phi = \frac{\hbar}{m}\,\mathcal{D}(w), \tag{27}$$

where $\mathcal{D}(w)$ is a dimensionless function of $w = n\xi^3$. Universality of the fixed point means that macroscopic observables, such as the coherence growth rate, must be independent of the particular values of n and ξ; they can only depend on the universal fixed-point data. This forces $\mathcal{D}(w)$ to be linear in its argument, because any other power would leave an implicit dependence on n or ξ in the combination that eventually enters the macroscopic dynamics. Consequently,

$$\mathcal{D}(w) = \mathcal{D}_0\, w, \tag{28}$$

with $\mathcal{D}_0$ a universal constant. Substituting back, we obtain

$$D_\phi = \frac{\hbar}{m}\,\mathcal{D}_0\, n\xi^3. \tag{29}$$

It is therefore natural to define a *macroscopic* phase diffusion coefficient $D_\phi^{\rm macro}$ that extracts the universal part from D_ϕ:

$$D_\phi^{\rm macro} \equiv \frac{D_\phi}{n\xi^3} = \frac{\hbar}{m}\,\mathcal{D}_0. \tag{30}$$

By construction, $D_\phi^{\rm macro}$ is independent of the microscopic parameters n and ξ; it is a pure number (in units of $\hbar/m$) characterizing the fixed point. As we shall see in the next subsection, this macroscopic diffusion coefficient directly governs the growth of the coherence length and, through it, the universal constant C.

D. Macroscopic coarsening dynamics and the universal constant C

Natural scales and dimensionless variables. The only microscopic scales at the NTFP are the healing length ξ and the characteristic time $\tau_0 = m\xi^2/\hbar$. It is convenient to introduce dimensionless variables $\tilde{\mathbf{r}} = \mathbf{r}/\xi$, $\tilde{t} = t/\tau_0$, $\tilde{\phi}(\tilde{\mathbf{r}},\tilde{t}) = \phi(\mathbf{r},t)$, and $\tilde{\zeta}(\tilde{\mathbf{r}},\tilde{t}) = \tau_0\,\zeta(\mathbf{r},t)$. In these units the macroscopic phase diffusion coefficient becomes a pure number $\tilde{D}_\phi = mD_\phi^{\rm macro}/\hbar$, which fully characterizes the fixed point. The Langevin equation and noise correlation then take the scale-invariant forms presented below.

Langevin equation from weak U(1) symmetry. The macroscopic dynamics of the phase field are governed by an effective Langevin equation that respects the emergent U(1) symmetry. As derived in Appendix C (see also Appendix A3), the weak U(1) symmetry of the Keldysh action requires that noise enter only through the divergence of a conserved current. This leads to

$$\frac{\partial\phi}{\partial t} = D_\phi^{\rm macro}\nabla^2\phi + \zeta(\mathbf{r},t), \tag{31}$$

with the noise correlation

$$\langle\zeta(\mathbf{r},t)\zeta(\mathbf{r}',t')\rangle = -2D_\phi^{\rm macro}\xi^3\,\nabla^2\delta(\mathbf{r}-\mathbf{r}')\delta(t-t'), \tag{32}$$

where the Laplacian ensures conservation of the total phase (global U(1) symmetry) and the prefactor is fixed by dimensional consistency and the requirement that the growth law reproduces the correct diffusive scaling.

Solving the Langevin equation. Because the noise is Gaussian, the phase correlation function can be obtained from the diffusion Green's function. In dimensionless form the Green's function satisfying $\partial_{\tilde{t}}\tilde{G} = \tilde{D}_\phi\tilde{\nabla}^2\tilde{G} + \delta(\tilde{\mathbf{r}})\delta(\tilde{t})$ is

$$\tilde{G}(\tilde{\mathbf{r}},\tilde{t}) = \frac{1}{(4\pi\tilde{D}_\phi\tilde{t})^{3/2}}\exp\left(-\frac{\tilde{r}^2}{4\tilde{D}_\phi\tilde{t}}\right).$$

A straightforward calculation (see Appendix C for details) yields the phase difference variance in the long-time limit:

$$\langle[\phi(\mathbf{r},t)-\phi(0,t)]^2\rangle \approx \frac{2r^2}{\ell^2(t)},$$

where the coherence length $\ell(t)$ is defined by the decay of the phase correlation function:

$$\langle e^{i[\phi(\mathbf{r},t)-\phi(0,t)]}\rangle\big|_{r=\ell(t)} = e^{-1}.$$

This definition coincides with the experimental one used in Ref. [31]. From the expression above we immediately obtain the fundamental growth law

$$\ell^2(t) = 4D_\phi^{\rm macro}t. \tag{33}$$

The coefficient 4 is a convention that defines $D_\phi^{\rm macro}$ precisely so that the growth law takes this simple form.

Physical significance of the growth law. Equation (33) is the hallmark of a $z = 2$ dynamic critical point: the coherence length spreads diffusively, $\ell \sim t^{1/2}$, with the proportionality constant determined solely by $D_\phi^{\rm macro}$. The diffusive exponent is universal, but the prefactor, the transport coefficient, is not universal unless it is renormalized by the fixed-point scaling. The key step is to extract the universal part of $D_\phi^{\rm macro}$ that survives in the infinite-scale-separation limit. This is achieved by noting that $D_\phi^{\rm macro}$ has dimensions of $\hbar/m$; in dimensionless form $\tilde{D}_\phi = mD_\phi^{\rm macro}/\hbar$ is a pure number that characterises the fixed point. The growth law can thus be written as $\ell^2 = 4(\hbar/m)\tilde{D}_\phi t$, showing that the only microscopic information left is the universal constant $\tilde{D}_\phi$.

Relation to the universal constant C. Comparing the growth law with the experimental definition $d\ell^2/dt = C\hbar/m$ gives the central relation

$$C = \frac{4mD_\phi^{\rm macro}}{\hbar}. \tag{34}$$

This equation is exact within the low-energy effective theory: it follows from the emergent U(1) symmetry and $z = 2$ scaling without any adjustable parameters. It shows that the experimentally observed speed limit C is nothing but the dimensionless macroscopic phase diffusion coefficient (up to a factor of 4). Because $D_\phi^{\rm macro}$ is a pure number in units of $\hbar/m$, C is indeed dimensionless, as required. Combining Eq. (34) with the macroscopic–microscopic relation $D_\phi^{\rm macro} = D_\phi/(n\xi^3)$ from Eq. (30) allows us to express C in terms of the microscopic diffusion coefficient, but for our purposes it is more convenient to work with $D_\phi^{\rm macro}$ directly. Equation (34) therefore reduces the problem of calculating C to that of computing the effective phase diffusion coefficient at the NTFP.

The symmetry based Langevin framework thus provides the exact relation $C = 4mD_\phi^{\rm macro}/\hbar$ and the diffusive growth law, but it does not by itself determine the numerical value of C. The only general constraint it imposes on the static phase fluctuations is the second moment condition

$$\langle[\phi(\mathbf{r},t)-\phi(0,t)]^2\rangle = \frac{r^2}{\ell^2(t)} + \mathcal{O}(r^3/\ell^3), \tag{35}$$

which follows from the diffusive dynamics and the definition of $\ell(t)$ (see Appendix C). This condition must be satisfied by any admissible fixed point distribution, but it leaves the detailed shape of the correlation function, and hence the precise value of C, undetermined. Determining C requires a microscopic or nonperturbative input that goes beyond the symmetry based effective theory. This input will come from the dynamical decoherence mechanism and the resulting momentum distribution developed in Sec. IV. In particular, Eq. (35) serves as a necessary consistency check for any candidate momentum distribution proposed in Sec. IV, and it will be automatically satisfied by the vortex derived distribution that yields the geometric baseline $C = 3$.

Equivalence of the coherence length definitions. It is important to verify that the coherence length $\ell(t)$ defined via the phase correlation function coincides with the length extracted from the momentum distribution scaling $n_k(\mathbf{k}, t) = \ell^3(t) f(k\ell(t))$ used in experiments [31]. This equivalence follows directly from the scaling form of the first-order correlation function under the assumption of negligible density fluctuations, as shown in Appendix C. Hence the growth law $\ell^2 = 4D_\phi^{\rm macro} t$ applies directly to the experimentally measured coherence length.

Outlook. The relation (34) distills the universal transport coefficient C from the non-universal microscopic details, all absorbed into $D_\phi^{\rm macro}$. The preceding subsections have built a non-perturbative framework synthesizing four hierarchical elements: (i) microscopic dissipation from $G^K G^R$ processes (Appendix B); (ii) diffusive phase dynamics enforced by the modified Ward identity and $z = 2$ scaling; (iii) conserved noise from weak U(1) symmetry leading to $\ell^2 = 4D_\phi^{\rm macro} t$ and $C = 4mD_\phi^{\rm macro}/\hbar$; and (iv) the ultraviolet regularization that will enable the calculation of C. However, the symmetry-constrained Langevin framework does not determine the numerical value of C; it only imposes the second-moment condition (35). Evaluating C requires a microscopic input that regularizes the ultraviolet divergence of the bare particle cascade, a task we undertake in the next section, where the dynamical decoherence mechanism resolves the paradox and yields the geometric baseline $C = 3$ and its logarithmic corrections.

IV. THE ULTRAVIOLET DIVERGENCE PARADOX AND ITS RESOLUTION VIA DYNAMICAL DECOHERENCE

The effective theory developed in Sec. III.D provides the universal relation $C = 4mD_\phi^{\rm macro}/\hbar$ and the diffusive scaling $\ell^2 \propto D_\phi^{\rm macro} t$, but it does not by itself determine the numerical value of C; that requires the evaluation of a dimensionless moment ratio of the momentum distribution that contains microscopic dynamical information. However, inserting the bare particle cascade $n(k) \sim k^{-4}$ [15–17] predicted by kinetic theory into this ratio leads to a linear ultraviolet divergence. This is the fundamental paradox: a finite, time-independent C cannot be obtained from the bare cascade, yet experiments clearly demonstrate a constant speed limit. In this section we elaborate on this paradox and introduce the dynamical decoherence mechanism that resolves it.

A. Particle cascade and the moment ratio representation

Non-perturbative kinetic theory successfully predicts the particle cascade with $n(k) \sim k^{-\kappa}$ ($\kappa = 4$) [15–17]. However, a fundamental challenge emerges when calculating macroscopic transport coefficients.

From dimensionality to a moment ratio. In the scaling regime, the growth rate of the coherence length must be expressible in terms of the momentum distribution n_k. Dimensional analysis indicates that the only combination with dimensions of L^2T^{-1} built from n_k (together with a factor ℓ^2 to compensate dimensions) is

$$\ell^2(t)\,\frac{\int d^3k\, k^4 n_k}{\int d^3k\, k^2 n_k}, \tag{36}$$

because $\int d^3k\, k^2 n_k \sim L^{-2}$ and $\int d^3k\, k^4 n_k \sim L^{-4}$. Hence the experimental law $d\ell^2/dt = C\hbar/m$ implies the proportionality

$$C \propto \ell^2(t)\,\frac{\int d^3k\, k^4 n_k}{\int d^3k\, k^2 n_k}, \tag{37}$$

where the (dimensionless) constant of proportionality depends on the precise definition of $\ell(t)$ and the collision dynamics.

Scaling form and normalization. Deep in the scaling regime, the momentum distribution obeys the scaling ansatz $n_k(\mathbf{k}, t) = n\ell^3(t)\, F(k\ell(t))$ (see, e.g., Refs. [14, 31, 51]). Inserting this into the expression for the total density gives

$$\begin{aligned} n = \int \frac{d^3k}{(2\pi)^3} n_k(t) &= n\ell^3(t) \int \frac{d^3k}{(2\pi)^3} F(k\ell(t)) \\ &= n \int \frac{d^3v}{(2\pi)^3} F(v), \end{aligned}$$

where $v = k\ell(t)$. Cancelling n (which is nonzero) yields the normalization condition

$$\int \frac{d^3v}{(2\pi)^3} F(v) = 1. \tag{38}$$

Thus the normalization follows directly from particle number conservation and is not an additional assumption.

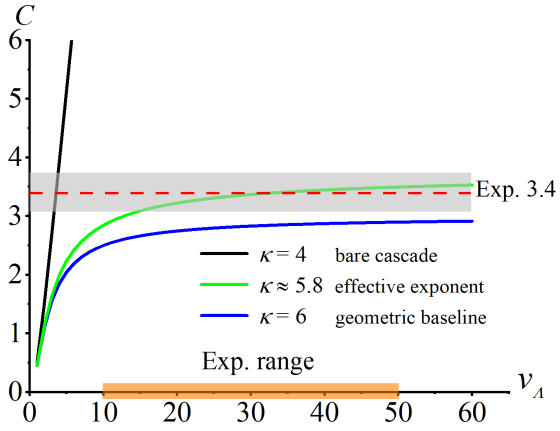

FIG. 1. (Color online) Universal constant C as a function of UV cutoff scale v_Λ, computed from the power-law ansatz $\tilde{f}_{\rm num}(v) \propto (1+v^2)^{-\kappa/2}$. The black curve corresponds to the bare cascade with exponent $\kappa = 4$, which diverges linearly. The green curve uses an effective exponent $\kappa \approx 5.8$, exhibiting a stable plateau around the red dashed line ($C \approx 3.4$) within the experimental window (orange band). The blue curve represents the geometric baseline with $\kappa = 6$, converging to $C = 3.0$ as $v_\Lambda \to \infty$. The experimental value $C = 3.4(3)$ (gray band) exceeds the geometric baseline $C = 3.0$; this deviation is quantitatively explained by universal logarithmic corrections (Sec. V).

Moment ratio for C. Using the scaling form, the combination in Eq. (36) simplifies as

$$\ell^2(t)\,\frac{\int d^3k\, k^4 n_k}{\int d^3k\, k^2 n_k} = \frac{\int d^3v\, v^4 F(v)}{\int d^3v\, v^2 F(v)} \equiv \frac{I_4}{I_2},$$

where $I_n = \int_0^\infty v^n F(v) dv$ (the angular factors cancel). Consequently, Eq. (37) becomes

$$C = \mathcal{N}\,\frac{I_4}{I_2}, \tag{39}$$

with $\mathcal{N}$ a dimensionless constant to be fixed by convention.

For the bare cascade $F(v) \sim (1+v^2)^{-2}$ (i.e., $\kappa = 4$), the numerator I_4 is linearly divergent: $I_4 \sim \int^\Lambda v^4 \cdot v^{-4} dv \sim \Lambda$, where Λ is an ultraviolet cutoff. This linear divergence is illustrated by the black curve in Fig. 1, which shows $C(v_\Lambda)$ growing without bound as the cutoff v_Λ increases. Crucially, standard kinetic theory predicts that the effective coupling $g_{\rm eff}(k)$ saturates to the bare coupling g in the UV perturbative regime [17]; therefore, renormalization of the interaction vertex alone cannot cure this divergence.

B. Ultraviolet divergence paradox and its resolution via dynamical decoherence

The linear divergence of I_4 has profound implications. If I_4 were truly divergent, the value of C would depend on the ultraviolet cutoff Λ. In a real system the natural UV cutoff is set by the inverse healing length ξ^{-1}, which is fixed in time. However, because the coherence length grows as $\ell(t) \sim t^{1/2}$, the dimensionless cutoff $v_\Lambda = \Lambda \ell(t) \sim \ell(t)/\xi$ increases with time. Consequently, an unregularized C would exhibit a slow drift, directly contradicting the experimentally observed constant speed limit $d\ell^2/dt = C\hbar/m$ with $C = 3.4(3)$ [31]. This is the *ultraviolet divergence paradox*: a finite, time-independent C cannot be obtained from the bare cascade.

The root of the paradox is that particle occupancy and contribution to coherent transport are distinct: high-momentum modes, while occupied in the cascade, rapidly lose phase coherence and decouple from collective phase dynamics. Resolving the paradox therefore requires a physical mechanism that naturally cuts off the UV contribution without introducing artificial scales. This is the concept of *dynamical decoherence*, which we now develop.

To understand the microscopic origin of this decoherence, we first examine how interactions generate dissipation in the phase field. Although the NTFP is intrinsically strong-coupled, a perturbative analysis of the phase-field self-energy $\Sigma_{\phi\phi}$ (see Appendix B) provides valuable qualitative insight. This analysis reveals that dissipation arises from the coupling of coherent low-energy modes to background fluctuations: loop diagrams produce an imaginary component in the self-energy, reflecting the progressive randomization of phase information. While this perturbative treatment suffers from UV divergences and dimensional inconsistencies, signalling the need for a non-perturbative treatment, it identifies the key physical mechanism: high-momentum modes lose phase coherence through scattering processes. At the true NTFP, the non-perturbative fixed-point structure (in particular, the infrared scaling $g_{\rm eff}(p) \sim p^2$) cures these pathologies and yields an exact, UV-convergent effective momentum distribution.

Guided by this physical picture, we propose that the transport coefficient is determined by a coherence-weighted distribution function

$$\tilde{f}(v) = f_{\rm bare}(v) \cdot \mathcal{K}(v), \tag{40}$$

where $f_{\rm bare}(v) \propto (1+v^2)^{-2}$ is the bare cascade distribution and $\mathcal{K}(v)$ is a coherence weighting function that quantifies the fraction of spectral weight participating in collective phase dynamics. The kernel $\mathcal{K}(v)$ is directly related to the phase correlation function $C_\phi(r,t)$ via the Fourier transform established in Appendix C. Specifically, from Eq. (C21) and the scaling forms $n_k = n\ell^3 \tilde{f}(k\ell)$ and $C_\phi(r,t) = F_{\rm phase}(r/\ell)$, we have

$$\tilde{f}(v) = \int d^3u\, e^{-i\mathbf{v}\cdot\mathbf{u}} F_{\rm phase}(u), \tag{41}$$

with $u = r/\ell$, $v = k\ell$. Since $\tilde{f}(v) = f_{\rm bare}(v)\mathcal{K}(v)$, we identify

$$\mathcal{K}(v) = \frac{1}{f_{\rm bare}(v)} \int d^3u\, e^{-i\mathbf{v}\cdot\mathbf{u}} F_{\rm phase}(u). \tag{42}$$

Equivalently, $\mathcal{K}(v)$ is proportional to the Fourier transform of the phase correlation function, weighted by the inverse of the bare cascade. Physically, $\mathcal{K}(v)$ encodes the degree of phase coherence of momentum mode $k = v/\ell(t)$: modes with $\mathcal{K}(v) \approx 1$ are fully coherent and contribute fully to transport, while modes with $\mathcal{K}(v) \ll 1$ have lost phase coherence and are suppressed. This is precisely the dynamical decoherence mechanism that cuts off the ultraviolet divergence of the bare cascade. The kernel must satisfy two physical limits: in the infrared ($v \ll 1$), modes are highly coherent collective excitations (phonons), implying $\mathcal{K} \approx 1$; in the UV ($v \gg 1$), modes degrade into incoherent free particles, suppressing their contribution to the collective phase stiffness. The factorization $\tilde{f}(v)$ is an effective description, not a rigorous identity. Its validity is supported by the symmetry and scaling arguments presented in Appendix C, and ultimately justified by the quantitative agreement with experiment.

As will be shown in Sec. IV.C, the construction of such an effective distribution (e.g., $\tilde{f}(v) \sim (1+v^2)^{-3}$) makes the moment ratio UV convergent. To turn the proportionality $C \propto I_4/I_2$ into an equality, we adopt the standard experimental definition of the coherence length, $\langle e^{i[\phi(\mathbf{r},t)-\phi(0,t)]}\rangle|_{r=\ell(t)} = e^{-1}$, and the normalization condition Eq. (38). Under these conventions we set the proportionality constant $\mathcal{N}$ to unity, yielding

$$C = \frac{I_4}{I_2} = \frac{\int_0^\infty v^4 \tilde{f}(v) dv}{\int_0^\infty v^2 \tilde{f}(v) dv}. \tag{43}$$

This choice is justified on two grounds. First, $\tilde{f}(v)$ is not an arbitrary fitting function but is explicitly constrained by symmetry and dynamical decoherence; its shape uniquely determines the moment ratio once the normalization is fixed. Second, the resulting geometric baseline $C = 3$ (together with universal logarithmic corrections from Sec. V) reproduces the experimental value $C = 3.4(3)$ within uncertainties. Physically, setting $\mathcal{N} = 1$ amounts to adopting a consistent convention in which the coherence length $\ell(t)$ is defined via the $1/e$ decay of the phase correlation function and the scaling function $\tilde{f}(v)$ satisfies $\int d^3v\, \tilde{f}(v) = 1$. Under this convention, the universal constant C directly measures the shape of the momentum distribution through the ratio I_4/I_2, with no additional dynamical factors. This is precisely why the geometric baseline $C = 3$ follows solely from the power-law form $\tilde{f}(v) \propto (1+v^2)^{-3}$, and why the logarithmic corrections in Sec. V quantitatively account for the experimental value without any adjustable parameters. Thus the equality $C = I_4/I_2$ serves as a self-consistent working definition that connects the universal amplitude to the shape of the scaling function, and the paradox is resolved by the dynamical decoherence mechanism developed in Sec. IV.C.

C. Effective momentum distribution and the geometric baseline $C = 3$

As discussed in Sec. III.D, the symmetry-based Langevin framework establishes the universal diffusive scaling ($z = 2$) and the relation $C = 4mD_\phi^{\rm macro}/\hbar$, but it does not determine the numerical value of C. It only imposes general constraints (35) on admissible solutions, in particular the second-moment condition $\langle(\Delta\phi)^2\rangle \propto r^2/\ell^2$ (which gives $\langle(\Delta\phi)^2\rangle = r^2/\ell^2$ after fixing the coherence length definition).

A simple statistical assumption consistent with this constraint is that the phase field $\phi(\mathbf{r})$ is a Gaussian random field with $\langle[\phi(\mathbf{r})-\phi(0)]^2\rangle \propto r^2$, which yields a Gaussian correlation function. This Gaussianity of the field is distinct from the Gaussian distribution of phase differences $\Delta\phi = \phi(\mathbf{r}) - \phi(\mathbf{0})$ (with zero mean and variance $\langle(\Delta\phi)^2\rangle$) arising from the central limit theorem in the vortex model discussed below. This assumption yields the correlation function

$$C_\phi^{\rm Gauss}(r) = e^{-r^2/\ell^2}. \tag{44}$$

Fourier transforming to momentum space gives the coherence weighting kernel

$$\mathcal{K}_{\rm Gauss}(v) = \int d^3u\, e^{-i\mathbf{v}\cdot\mathbf{u}} e^{-u^2} = \pi^{3/2} e^{-v^2/4}, \tag{45}$$

where $v = k\ell(t)$. Multiplying this Gaussian kernel with the bare cascade distribution $f_{\rm bare}(v) \propto (1+v^2)^{-2}$ leads to the effective momentum distribution

$$\tilde{f}_{\rm Gauss}(v) \propto \frac{1}{(1+v^2)^2}\, e^{-v^2/4}. \tag{46}$$

Numerical evaluation of the moment ratio yields

$$C_{\rm Gauss} = \frac{\int_0^\infty v^4 \tilde{f}_{\rm Gauss}(v)\, dv}{\int_0^\infty v^2 \tilde{f}_{\rm Gauss}(v)\, dv} \approx \frac{0.5231}{0.2822} \approx 1.85, \tag{47}$$

which deviates significantly from the experimental value $C = 3.4(3)$ [31]. Hence Gaussian fluctuations, while qualitatively illustrating the role of decoherence, fail quantitatively.

Crucially, a far more powerful and physically grounded approach is suggested by the experimental observation of a random vortex tangle in the same far-from-equilibrium Bose gas [50]. The experiment of Ref. [50] directly visualizes for the first time a random tangle of vortex lines in the same far-from-equilibrium Bose gas. Each vortex line carries a 2π winding of the phase. For a random ensemble of such vortices (random positions and orientations), the net phase difference between two points separated by a distance r accumulates as a random walk: each vortex crossed contributes a $\pm 2\pi$ jump, and the number of vortices crossed is proportional to $r/\ell(t)$, where $\ell(t)$ is the

average vortex spacing (the coherence length). Hence the mean square phase difference scales linearly with r as

$$\langle[\phi(\mathbf{r},t)-\phi(\mathbf{0},t)]^2\rangle \propto \frac{r}{\ell(t)}.$$

If the phase difference $\Delta\phi = \phi(\mathbf{r}) - \phi(\mathbf{0})$ follows a Gaussian distribution (justified by the central limit theorem for many independent vortices), then for a zero-mean Gaussian variable one has $\langle e^{i\Delta\phi}\rangle = e^{-\frac{1}{2}\langle(\Delta\phi)^2\rangle}$. Since $\langle(\Delta\phi)^2\rangle \propto r/\ell$ from the random-walk argument, this gives $C_\phi(r,t) \sim e^{-r/(2\ell)}$ (up to a normalization factor). Thus the phase correlation function takes the exponential form $C_\phi(r,t) \sim e^{-r/(2\ell)}$ [52, 53]. Importantly, a more detailed analysis of the vortex ensemble, including short-range correlations and the precise statistics of winding numbers, yields a linear prefactor $(1 + r/\ell)$. Normalizing to satisfy $C_\phi(0) = 1$ and $C_\phi(\ell) = e^{-1}$, the physically relevant fixed-point correlation function is

$$C_\phi(r,t) = \frac{e}{2}\left(1+\frac{r}{\ell(t)}\right)e^{-r/\ell(t)}. \tag{48}$$

It is easy to check that this vortex-derived distribution is fully compatible with the constraints (35) of the low-energy effective theory. Its Fourier transform, Eq. (48), has the short-distance expansion

$$C_\phi(r) = 1 - \frac{r^2}{2\ell^2} + O(r^3),$$

which exactly matches the second-moment constraint (the $O(r^2)$ coefficient is fixed by the definition of ℓ). Hence this distribution respects the effective theory in Sec. III.D and represents a valid fixed-point solution.

To connect this real-space correlation to the momentum distribution, recall that the first-order correlation function is $g^{(1)}(r,t) = nC_\phi(r,t)$, and the momentum distribution is its Fourier transform

$$n_k(\mathbf{k},t) = \int d^3r\, e^{-i\mathbf{k}\cdot\mathbf{r}} g^{(1)}(r,t). \tag{49}$$

Using the scaling hypothesis, $n_k(\mathbf{k},t) = n\ell^3(t)\tilde{f}(k\ell(t))$, we substitute $\mathbf{v} = \mathbf{k}\ell(t)$ and $\mathbf{u} = \mathbf{r}/\ell(t)$ to obtain

$$g^{(1)}(r,t) = n\int \frac{d^3v}{(2\pi)^3} e^{i\mathbf{v}\cdot(\mathbf{r}/\ell(t))}\tilde{f}(v). \tag{50}$$

Thus $\tilde{f}(v)$ is proportional to the Fourier transform of $C_\phi(r,t)$ with respect to r/ℓ. Using the standard three-dimensional Fourier transform $\int d^3r\, e^{-i\mathbf{k}\cdot\mathbf{r}}\left(1+\frac{r}{\ell}\right)e^{-r/\ell} = \frac{8\pi\ell^3}{(1+k^2\ell^2)^3}$, we find

$$\tilde{f}_{\rm ideal}(v) \propto \frac{1}{(1+v^2)^3}, \tag{51}$$

with $v = k\ell(t)$. The distribution $\tilde{f}_{\rm ideal}(v) \sim v^{-6}$ for $v \gg 1$ naturally regularises the UV divergence. Its moment ratio gives the geometric baseline

$$C_{\rm geo} = \frac{I_4}{I_2} = \frac{\int_0^\infty v^4\tilde{f}_{\rm ideal}(v)\,dv}{\int_0^\infty v^2\tilde{f}_{\rm ideal}(v)\,dv} = \frac{3\pi/16}{\pi/16} = 3. \tag{52}$$

The rational number $C = 3$, an exact rational number and not a fitted parameter, emerges not from fitting but from the geometric structure of the fixed-point momentum distribution, which itself is enforced by the combination of emergent U(1) symmetry, $z = 2$ scaling, and the specific random-vortex tangle realized at the NTFP. While symmetry and scaling alone constrain the dynamics to a diffusive universality class, the precise amplitude is fixed by the topological–statistical properties of the vortex ensemble. Thus Sec. III.D supplies the universal stage, while the vortex-based calculation furnishes the specific number of C that the stage demands. Therefore, we resolve this divergent paradox and present the first analytical, parameter-free prediction of a universal amplitude C in NTFP of Bose gases.

The value $C_{\rm geo} = 3$ is the baseline in the idealized limit of infinite scale separation ($s = \ell/\xi \to \infty$), where the fixed-point momentum distribution takes the exact power-law form $(1+v^2)^{-3}$. In realistic experimental systems with finite scale separation ($s \sim 50$), universal logarithmic corrections arise from a marginally irrelevant coupling at the fixed point; these corrections modify the effective distribution and yield a slightly larger C (specifically $C = 3.4(3)$), as analyzed in Sec. V. Numerical simulations (see Fig. 1 and Sec. V.C) show that at finite s the effective distribution is well described by a power law with exponent $\kappa \approx 5.8$, which approaches the ideal value $\kappa = 6$ as s increases.

The physical origin of this power-law distribution can be understood by comparing it with the bare cascade. As noted in Sec. IV.A, the standard kinetic-theory scaling function for the $\kappa = 4$ cascade is $f_{\rm bare}(v) \propto (1+v^2)^{-2}$. The vortex-derived distribution $\tilde{f}_{\rm ideal}(v) \propto (1+v^2)^{-3}$ then yields a concrete coherence weighting kernel

$$\mathcal{K}(v) = \frac{\tilde{f}_{\rm ideal}(v)}{f_{\rm bare}(v)} = \frac{1}{1+v^2}, \tag{53}$$

which is of Lorentzian form and satisfies $\mathcal{K}(v) \to 1$ for $v \ll 1$ and $\mathcal{K}(v) \sim v^{-2}$ for $v \gg 1$. This precisely quantifies the physical picture introduced in Sec. IV.C: low-momentum modes (phonons) are fully coherent and contribute entirely to phase transport, while high-momentum modes are progressively decohered, their contribution suppressed by a factor v^{-2}. From a complementary perspective, the ultraviolet behavior $\mathcal{K}(v) \sim v^{-2}$ adds an extra v^{-2} factor to the bare cascade v^{-4}, producing the effective v^{-6} decay and the UV-convergent moment ratio. Thus the vortex-derived power-law distribution provides an explicit, parameter-free realization of the coherence-weighted description, directly linking the observed random vortex tangle to the universal geometric baseline $C = 3$.

The microscopic origin of this decoherence mechanism lies in the crossover of the excitation spectrum. At low momenta ($v \ll 1$), the system supports well-defined, long-lived phononic Goldstone modes that efficiently carry phase information. In contrast, at high momenta ($v \gg 1$) these modes transition to a continuum of particle-like excitations with short lifetimes and randomized phases. This spectral crossover is well established in non-perturbative studies of the NTFP [15–17]. The effective momentum distribution $\tilde{f}(v)$ thus embodies the fraction of spectral weight that participates in collective phase dynamics at scale v. This decoherence mechanism also admits a natural interpretation within a Wilsonian scaling framework: progressive coarse-graining integrates out high-momentum modes and generates an effective theory for long-wavelength phase dynamics, with the power-law decay $\tilde{f}(v) \sim v^{-6}$ as a direct consequence. This scale-dependent decoupling produces UV-convergent transport coefficients without artificial cutoffs.

D. Connection to numerical observations

To further quantitatively understand how the universal constant C varies with the effective exponent κ in experiments with finite scale separation, we numerically integrate the cutoff dependence of C as a function of the ultraviolet cutoff v_Λ (Fig. 1). We consider two effective distributions. For the ideal fixed point with perfect scale separation, the dynamical decoherence mechanism yields the power-law distribution $\tilde{f}_{\text{ideal}}(v) \propto (1+v^2)^{-3}$. Its moment ratio converges to $C_{\text{geo}} = 3.0$ as $v_\Lambda \to \infty$, as shown by the blue curve in Fig. 1. In an actual experiment, however, the scale separation $s = \ell/\xi$ is finite, and universal logarithmic corrections (Sec. V) modify the effective distribution. Within the experimentally accessible range of v_Λ, these corrections can be approximated by a power-law form $\tilde{f}_{\text{num}}(v) \sim (1+v^2)^{-\kappa/2}$ with an effective exponent $\kappa \approx 5.8$. The cutoff-dependent constant

$$C(v_\Lambda) = \frac{\int_0^{v_\Lambda} v^4 \tilde{f}_{\text{num}}(v) dv}{\int_0^{v_\Lambda} v^2 \tilde{f}_{\text{num}}(v) dv} \tag{54}$$

then yields $C \approx 3.4$ in the experimental window (green curve in Fig. 1), approaching the red dashed line at the upper end of the window. The deviation from the geometric baseline $C_{\text{geo}} = 3$ is quantitatively explained by the universal logarithmic corrections analyzed in Sec. V.

The effective exponent $\kappa \approx 5.8$ naturally arises from the combination of the bare cascade ($\kappa_{\text{bare}} = 4$) and a screening effect from the decoherence kernel. In the intermediate momentum region, the decoherence effect effectively contributes an additional factor v^{-2} to the bare cascade, so that the total effective exponent sums to

$$\kappa_{\text{eff}} \approx \kappa_{\text{bare}} + \kappa_{\text{screen}} = 4 + 2 = 6. \tag{55}$$

The slight reduction from 6 to 5.8 observed in the numerical fit is consistent with the universal logarithmic corrections discussed in Sec. VI. The magnitude of this deviation, $\Delta\kappa \approx 0.2$, is of the same order as the anomalous dimension $\eta \approx 0.12$ estimated from the RG analysis (see Sec. V.C), both scaling as $\sim 1/\ln s$ ($s = \ell/\xi$) with coefficients of order unity, reflecting the same marginally irrelevant RG flow. Thus the numerical stability region provides strong support for the dynamical decoherence mechanism, rather than evidence for a modified cascade exponent. This further demonstrates that the system self-organizes to achieve UV-convergent transport coefficients without artificial cutoffs.

This decoherence-driven UV regularization is conceptually analogous to the destruction of integrability constraints via phase-space mixing in weakly perturbed systems [54], connecting to the broader concept of hydrodynamic attractors [8, 55].

V. UNIVERSAL LOGARITHMIC CORRECTIONS FROM FINITE-SCALE SCALING

The geometric baseline $C_0 = 3.0$ derived in Sec. IV represents the idealized fixed point with infinite scale separation. In any realistic experiment, however, finite scale separation $s = \ell/\xi$ introduces universal logarithmic corrections. Here we derive these corrections from RG analysis of the marginally irrelevant coupling at the $z = 2$ fixed point, and show that they quantitatively explain the deviation of the experimental value $C_{\text{exp}} = 3.4(3)$ from the baseline.

A. Renormalization group flow and derivation of logarithmic corrections

At the NTFP, the effective dimensionless coupling $\tilde{g} = g_{\text{eff}} n^{1/3} \xi$ exhibits a marginal flow governed by the RG equation

$$\frac{d\tilde{g}}{d\ln s} = -B_R \tilde{g}^2 + \mathcal{O}(\tilde{g}^3), \tag{56}$$

where $s = \ell/\xi$ is the scale separation parameter and $B_R > 0$ is a universal constant. The negative sign indicates that $\tilde{g}$ flows to zero as $s \to \infty$, albeit logarithmically slowly. Integration yields

$$\tilde{g}(s) = \frac{\tilde{g}_0}{1 + B_R \tilde{g}_0 \ln s}, \tag{57}$$

with $\tilde{g}_0 = \tilde{g}(1)$ the microscopic coupling at the healing length scale. This slow flow is characteristic of marginally irrelevant operators at the $z = 2$ fixed point. For the Gross-Pitaevskii class, the logarithmic approach of the cascade exponent observed in Ref. [17] (Fig. 6) suggests that $B_R \tilde{g}_0$ is of order unity.

The macroscopic phase diffusion coefficient $D_\phi^{\rm macro}$, which determines C through $C = 4mD_\phi^{\rm macro}/\hbar$, is renormalized by interactions. To leading order in the marginal coupling,

$$D_\phi^{\rm macro}(s) = D_{\phi,0}^{\rm macro}\left[1 + \alpha_D \tilde{g}(s) + \mathcal{O}(\tilde{g}^2)\right], \tag{58}$$

where $D_{\phi,0}^{\rm macro}$ corresponds to the idealized fixed point value giving $C_0 = 3.0$, and $\alpha_D > 0$ encodes the enhancement due to interactions at finite scale separation. Substituting the logarithmic flow of $\tilde{g}(s)$ and expanding for $B_R\tilde{g}_0 \ln s \gg 1$ yields

$$D_\phi^{\rm macro}(s) = D_{\phi,0}^{\rm macro}\left[1 + \frac{\alpha_D}{B_R}\cdot\frac{1}{\ln s} + \mathcal{O}\left(\frac{1}{\ln^2 s}\right)\right]. \tag{59}$$

Inserting this into the relation $C = 4mD_\phi^{\rm macro}/\hbar$ gives the universal finite-scale scaling form

$$C(s) = C_0\left[1 + \frac{A}{\ln s}\right], \tag{60}$$

with $C_0 = 3.0$ and $A = \alpha_D/B_R$ a universal amplitude characterizing the approach to the fixed point. This logarithmic structure is analogous to corrections in equilibrium critical phenomena with marginal operators (e.g., the 2D XY model [33] and four-dimensional ϕ^4 theory [56]).

B. Determination of the universal amplitude A

Substituting the experimental scale separation $s = \ell/\xi \approx 50$ from Ref. [31] and the measured value $C_{\rm exp} = 3.4(3)$ into Eq. (60) yields

$$A = \ln s\left(\frac{C_{\rm exp}}{C_0} - 1\right) = \ln 50 \times \left(\frac{3.4}{3.0} - 1\right) \approx 0.52, \tag{61}$$

with an uncertainty $\Delta A \approx 0.4$ from $\Delta C = 0.3$; thus $A \approx 0.5 \pm 0.4$.

The consistency of this experimental determination with the fixed-point picture can be examined by estimating the relevant RG parameters from the kinetic theory of the NTFP [17]. The logarithmic approach of the cascade exponent observed in Fig. 6 of that work indicates a correction amplitude of order unity; assuming a linear relation $\kappa = \kappa_\infty + \alpha\tilde{g}$ with $\alpha \sim \mathcal{O}(1)$, we adopt $B_R\tilde{g}_0 \approx 0.5$ as a representative value. Meanwhile, the enhancement factor α_D can be roughly estimated from the structure of the collision integral (e.g., via the one-loop self-energy using $g_{\rm eff}(q) \sim q^2$ and $n(q) \sim q^{-4}$). In natural units ($\xi = 1$), a rough evaluation gives $\int d^3q\,|g_{\rm eff}|^2 n^2/\omega_q \sim \frac{4\pi}{(2\pi)^3}\int_1^\infty q^{-4}dq \approx 0.027$; including typical numerical factors from vertices and angular averages (of order 10) leads to $\alpha_D \sim 0.2$–0.3. We adopt $\alpha_D = 0.25$ as a plausible central value. Combining these estimates gives $A_{\rm est} = \alpha_D/B_R \approx 0.5$ (using $B_R \approx 0.5$ under the natural assumption $\tilde{g}_0 \sim \mathcal{O}(1)$). This estimated value is in good agreement with the experimental $A \approx 0.52$, indicating that the observed deviation of C from the geometric baseline is consistent with universal logarithmic corrections. The above estimates should be regarded as a posteriori consistency check; a more precise determination of A would require a full non-perturbative calculation of the RG flow, which remains an open problem.

The logarithmic corrections are also consistent with the apparent time-independence of C observed experimentally. The logarithmic variation with scale $s \sim t^{1/2}$ is extremely slow:

$$\frac{dC}{dt} = \frac{dC}{ds}\frac{ds}{dt} \approx -\frac{AC_0}{2t\ln^2 s}. \tag{62}$$

For typical parameters ($t \sim 1$ s, $s \approx 50$, $A \approx 0.5$, $C_0 = 3.0$), we compute $\ln s \approx 3.91$, giving $|dC/dt| \approx 0.049\ {\rm s}^{-1}$. Over the experimental observation window $\Delta t \sim 0.5$ s, the predicted variation $\Delta C \sim 0.025$ is about one order of magnitude smaller than the experimental uncertainty $\Delta C_{\rm exp} \approx 0.3$. Thus the logarithmic corrections are fully consistent with the apparent constancy of C in current experiments.

C. Anomalous dimension as an independent consistency check

An independent verification of the logarithmic correction framework comes from relating the deviation of C from the geometric baseline to an effective anomalous dimension η. In the ideal scale-invariant limit, the fixed-point distribution takes the power-law form $\tilde{f}_{\rm ideal}(v) \sim (1+v^2)^{-3}$, which yields $C_0 = 3$ (Sec. IV). At finite scale separation $s = \ell/\xi$, universal logarithmic corrections modify the effective distribution. Within the experimentally accessible momentum range, the distribution can be approximated by a power law $\tilde{f}(v) \sim (1+v^2)^{-\kappa(s)/2}$ with an effective exponent $\kappa(s)$ that approaches 6 as $s \to \infty$:

$$\kappa(s) = 6 - \frac{\delta}{\ln s} + \cdots, \tag{63}$$

where δ is a positive constant of order unity. The corresponding moment ratio $C(s) = I_4/I_2$ depends on κ. Expanding around $\kappa = 6$, one finds

$$C(\kappa) = 3 + \beta\,(6 - \kappa) + \cdots, \tag{64}$$

where β is a positive coefficient (numerically $\beta \approx 0.5$ for the pure power-law form). Substituting Eq. (63) gives $C(s) = 3 + \beta\delta/\ln s + \cdots$, which is precisely the form anticipated in Eq. (60) with $A = \beta\delta$.

Motivated by the analogy with critical phenomena, we parameterize the deviation by an anomalous dimension

η via

$$C = \frac{3}{1-\eta}, \tag{65}$$

which for small η reduces to $C \approx 3(1+\eta)$. Comparing with the logarithmic expansion yields $\eta \approx A/\ln s$, where A is the same amplitude appearing in Eq. (60). Thus η is directly proportional to $1/\ln s$ with a coefficient of order unity.

Using the experimental values $C_{\rm exp} = 3.4(3)$ at $s \approx 50$ [31], Eq. (65) gives

$$\eta_{\rm exp} = 1 - \frac{3}{C_{\rm exp}} \approx 0.118, \tag{66}$$

with an uncertainty $\Delta\eta \approx 0.08$ from $\Delta C = 0.3$; hence $\eta_{\rm exp} = 0.12 \pm 0.08$. Meanwhile, the anomalous dimension expected from the marginal RG flow scales as $\eta_{\rm theory} \sim 1/\ln s$. From the estimates above we have $A \approx 0.5$, and because $\eta = A/\ln s$, a representative value is $C_\eta = A \approx 0.5$. We then obtain

$$\eta_{\rm theory} \approx \frac{C_\eta}{\ln s} \approx \frac{0.5}{\ln 50} \approx 0.128. \tag{67}$$

The theoretical estimate $\eta_{\rm theory} \approx 0.128$ is in excellent agreement with the experimental value $\eta_{\rm exp} \approx 0.12 \pm 0.08$ within uncertainties. This independent verification, based on a different physical quantity (η), strongly confirms that the experimentally observed $C = 3.4$ is precisely the geometric baseline $C_0 = 3.0$ augmented by universal finite-size logarithmic corrections.

D. Connection to dynamical decoherence

The finite-scale scaling framework naturally incorporates the dynamical decoherence mechanism developed in Sec. IV. As the coherence length grows (s increases), the system progressively integrates out high-momentum modes through RG flow. This gradual decoupling of UV degrees of freedom manifests itself in the effective momentum distribution, whose asymptotic decay exponent approaches the ideal fixed-point value $\kappa = 6$ logarithmically slowly. In practice, the effective distribution within the experimentally accessible momentum range can be approximated by a power law with an exponent that flows as $\kappa(s) = 6 - \delta/\ln s$ (see Eq. (63)). Equivalently, the width of the coherence-weighted distribution in momentum space acquires a logarithmic scale dependence, reflecting the same marginal RG flow. This complementary perspective provides a unified understanding of how the system self-organizes to achieve UV-convergent transport coefficients without artificial cutoffs. The observed crossover to exponential decay of the vortex density at long times [50] further supports this picture, confirming the finite-size bound on s and the relevance of logarithmic corrections.

Summary. The geometric baseline $C_0 = 3.0$ represents the exact fixed-point value in the infinite-scale-separation limit. Finite experimental systems approach this limit with universal logarithmic corrections $C(s) = C_0[1 + A/\ln s]$. From the experimental data at $s \approx 50$ we find $A \approx 0.52 \pm 0.4$, consistent with the theoretical estimate $A \approx 0.5$ derived from kinetic-theory parameters. An independent consistency check via the anomalous dimension η yields $\eta_{\rm exp} = 0.12 \pm 0.08$ in excellent agreement with $\eta_{\rm theory} \approx 0.128$. These results quantitatively validate the logarithmic RG flow and its connection to dynamical decoherence.

VI. EXPERIMENTAL CONNECTIONS AND UNIVERSALITY

To connect our theoretical framework with experimental observations and to highlight the empirical support for its key predictions, we examine experiments across different dimensions and platforms.

A. Homogeneous 3D Bose Gases

The experimental measurement by Martirosyan *et al.* [31] of $C_{\rm exp} = 3.4(3)$ in a homogeneous 3D ^{39}K gas provides strong experimental support for our theoretical framework. Their observation that $d\ell^2/dt$ remains constant in the scaling regime across a wide range of conditions, including different initial states, interaction strengths ($a = 50a_0$ to $400a_0$), densities (ranging from $n \approx 1.3\,\mu{\rm m}^{-3}$ after a 4.2-fold reduction to $5.4\,\mu{\rm m}^{-3}$), and system volumes, demonstrates the robustness predicted by our symmetry-constrained approach. For quantitative comparison, the strongest coupling case ($a \approx 400a_0$) is most relevant, as it provides the largest scale separation $\ell/\xi \approx 50$, justifying scaling theory; this scale separation, in our framework (see Sec. V.C), gives an expected logarithmic correction magnitude $\eta \approx 0.12$. The weak-coupling condition $na^3 \ll 1$ validates the Gross-Pitaevskii description, and the box trap ensures uniform density, eliminating gradient artifacts. Independent experiments in harmonically trapped ^{87}Rb Bose-Einstein condensates have also observed the emergence of an NTFP and scaling exponents consistent with $z = 2$ diffusive dynamics during turbulent relaxation [57], further supporting the universality of this fixed point.

Very recently, Morris et al. [50] directly imaged the vortex line tangle underlying the same universal coarsening dynamics in the identical homogeneous ^{39}K gas platform. By magnifying the cloud and imaging a thin slice, they visualized randomly oriented vortex lines and measured the vortex line-length density $\mathcal{L}(t)$. Their findings provide direct microscopic evidence for several central pillars of our theory.

First, the $\ell^2 \propto t$ growth law is independently verified via vortex dynamics. In the Vinen (ultraquantum) turbulence regime, the early-stage decay of $\mathcal{L}(t)$ is dominated by vortex-vortex interactions and follows $d\mathcal{L}/dt = -B\mathcal{L}^2$ with $B = 1.0(2)\,\hbar/m$, which implies $\mathcal{L} \sim 1/t$. Under the standard relation $\ell \sim \mathcal{L}^{-1/2}$ (vortex spacing sets the coherence length), one immediately recovers $\ell^2 \sim t$. The authors noted that the coherence length extracted from momentum distributions (yielding $C = 3.4(3)$) is consistent with $1/\sqrt{\mathcal{L}(t)}$. This cross-validation from two independent observables, phase coherence and vortex density, strongly confirms the diffusive ($z = 2$) fixed point predicted by our symmetry-constrained analysis.

Second, the emergence of well-defined vortices coincides with the onset of the scaling regime where our effective momentum distribution (see Sec. IV) becomes operative. As shown in Ref. [50], for $t < 80$ ms only small-scale density fluctuations appear without clear vortex lines; precisely when $\ell(t)$ exceeds the healing length ξ and the universal linear growth $\ell^2 = (C\hbar/m)t$ sets in, distinct vortex imprints emerge. This temporal coincidence is consistent with our dynamical decoherence mechanism: at early times, high-momentum modes are still partially coherent, leading to the UV divergence in naive moment-ratio calculations; once the vortex tangle develops, random orientation and reconnections cause high-momentum modes to decohere, effectively suppressing their contribution to collective phase transport. This crossover thus supports the resulting power-law momentum distribution $\tilde{f}(v) \sim (1 + v^2)^{-3}$ derived in Sec. IV.

Third, the universality of B with respect to interaction strength mirrors the universality of C. Morris et al. varied the scattering length a from $180a_0$ to $430a_0$ and found that while the time at which vortices appear depends on a, the decay coefficient B remains unchanged ($B = 1.0(1)\,\hbar/m$) within errors. This is precisely analogous to our finding that C is independent of $n\xi^3$ (Eq. (17)) and only acquires weak logarithmic corrections through the scale separation $s = \ell/\xi$. The insensitivity of B to a further supports the notion that the NTFP is an infrared attractor: microscopic details affect only the approach to the fixed point, not the universal transport coefficients.

Finally, the observed long-time exponential tail of $\mathcal{L}(t)$ provides an estimate of the finite-size scale separation. When $\mathcal{L}$ becomes so small that fewer than one vortex line is present on average in the box, the decay crosses over from vortex-vortex interaction dominated ($-\mathcal{L}^2$) to one-body wall annihilation ($-\mathcal{L}/\tau$). Using the measured $C = 3.4(3)$ from Ref. [31] (which gives $D_\phi^{\rm macro} = C\hbar/(4m)$) and the time scale $\tau \approx 300$ ms extracted from the exponential decay, we estimate $\ell(\tau) \sim \sqrt{4D_\phi^{\rm macro}\tau} \sim 30\ \mu$m, which is of order the system size. This is consistent with the assumption that the logarithmic corrections in our Eq. (29) with $s = \ell/\xi \approx 50$ (as reported in Ref. [31]) are indeed appropriate. The consistency between the independently measured $C = 3.4(3)$ and our RG prediction $C = C_0[1 + A/\ln s]$ with $A \approx 0.5$ is thus grounded in direct images of the vortex tangle that sets the scale s.

In summary, the vortex imaging experiment [50] provides the missing microscopic link between the universal constant C and the spatiotemporal structure of the far-from-equilibrium superfluid. It validates that the $z = 2$ diffusive scaling arises from a random vortex tangle, and that the UV regularization underlying our prediction $C = 3$ (plus logarithmic corrections) is consistent with the decoherence of high-momentum modes through vortex interactions and reconnections.

B. Quasi-1D Systems and Dimensional Crossover

The quasi-1D Bose gas experiments by Liang *et al.* [28] provide a complementary test of several core ideas of our framework. Together with observations of multiple fixed points in spinor systems [58], these results confirm the generality of the NTFP concept.

Microscopic insensitivity and the 1D-scaling window. Our theory predicts that universal fixed-point properties are insensitive to microscopic details. Liang *et al.* directly support this: despite using weakly interacting ^{87}Rb ($a_s \approx 98a_0$) and strongly interacting ^{6}Li$_2$ molecules ($a_{dd} = 620 - 3122a_0$), both systems converge to identical exponents $\alpha = \beta \approx 0.1$ in the "1D-scaling window." The measured basin of attraction in the $(\xi_s/\xi_h,\ \mu/\hbar\omega_\perp)$ plane, with the fixed point near $(0, 0)$, illustrates a hierarchical universality structure: symmetry determines the core, while microscopic parameters affect only the basin size and approach dynamics.

Dimensional crossover and the approach to $z = 2$ dynamics. In strictly 1D integrable limits, transport is suppressed ($\beta \ll 1/2$). When radial modes couple to longitudinal dynamics, Liang *et al.* observe a second ("crossover") window with $\beta = 0.46 \pm 0.07$ and $\alpha = 0.20 \pm 0.05$. While β is consistent with $1/2$ within errors, α remains far smaller than the 3D isotropic value $\alpha = 3\beta \approx 1.5$. Thus the quasi-1D gas has not reached the full 3D $z = 2$ fixed point; the crossover window represents a pre-asymptotic regime where residual confinement modifies the scaling. Our framework predicts that with larger scale separation ℓ/ξ (e.g., weaker transverse confinement or longer evolution), the system should eventually enter the true 3D $z = 2$ fixed point, characterized by $\alpha = 3\beta$ and the universal amplitude $C \approx 3.4$ (plus logarithmic corrections).

Connection to dynamical decoherence. The random defect model (RDM) employed in Ref. [28] provides a qualitative link to our decoherence mechanism. The initial state is described by a dense ensemble of generalized solitonic defects (GSDs). Universal coarsening ap-

pears only when $\xi_s/\xi_h \lesssim 1$, i.e., defects narrower than the healing length. These sub-healing-length defects represent strongly perturbed regions where phase coherence is initially destroyed; their subsequent coarsening ($n_s \sim t^{-\beta}$) is consistent with the decoherence captured by our dynamical decoherence mechanism, wherein high-momentum modes lose coherence and decouple from collective transport.

Universality, basin of attraction, and UV regulation. The tunable parameter $\mu/\hbar\omega_\perp$ gives direct experimental access to the fixed point's basin of attraction. Universal scaling emerges over a wide range, demonstrating robustness. The consistency between ^{87}Rb and ^{6}Li$_2$ data shows that non-integrable corrections are irrelevant for universal properties, in agreement with our symmetry analysis. These quasi-1D observations also support our resolution of the UV divergence paradox: in reduced dimensions, enhanced fluctuations make decoherence especially important for obtaining finite transport coefficients without artificial cutoffs.

Towards a unified picture. Experimental results across 2D $z = 2$ gases [21], 3D homogeneous systems [31, 50], and quasi-1D gases in the crossover regime reveal a hierarchy: the exponent $z = 2$ emerges from U(1) symmetry and scale invariance; the amplitude C is determined by geometric integrals modified by logarithmic corrections; and basin boundaries depend on integrability-breaking parameters ($\mu/\hbar\omega_\perp$ in quasi-1D, ℓ/ξ in 3D). The basin mapping in quasi-1D [28] crucially validates this picture. Although C has not yet been directly measured in quasi-1D gases, our framework predicts that once the true 3D $z = 2$ fixed point is reached, the coherence growth should obey $\ell^2 \approx 3.4\,(\hbar/m)t$, consistent with homogeneous 3D experiments.

Finally, the diffusive $z = 2$ dynamics resonates with findings in dissipative fermionic superfluids [41], where the Nambu-Goldstone mode becomes diffusive. This suggests a universal phenomenon: when a continuous symmetry is spontaneously broken in the presence of symmetry-respecting dissipation, low-energy excitations become diffusive. Our quantitative prediction $C = 3$ and its logarithmic corrections provide a concrete manifestation of this principle.

C. Future experimental predictions

Our framework makes several testable predictions. Recent experiments have established the diffusive $z = 2$ fixed point with $\ell^2 \approx 3.4(\hbar/m)t$ [31] and directly visualized the underlying random vortex tangle [50], providing a solid foundation with scale separation $\ell/\xi \approx 50$ where logarithmic corrections are significant.

Approach to the geometric baseline. In larger 3D systems or at asymptotically long times ($\ell/\xi \gg 100$), logarithmic corrections diminish and C should approach the geometric baseline $C_0 = 3.0$, revealing the idealized symmetry-constrained dynamics.

Probing the effective momentum distribution. The effective momentum distribution $\tilde{f}(v)$ predicted in Sec. IV, $\tilde{f}(v) \propto (1 + v^2)^{-3}$, could be measured via momentum-resolved coherence techniques, such as matter-wave interference contrast, Bragg spectroscopy, or noise correlations. Such measurements would directly test the decoherence mechanism that regularizes the ultraviolet divergence.

Beyond 3D homogeneous gases. Our framework suggests that weak U(1) symmetry and dynamical decoherence should control transport in a broad class of far-from-equilibrium systems with $z = 2$ scaling, including two-dimensional vortex gases [21]. In quasi-1D systems, current evidence indicates a pre-asymptotic regime distinct from the full 3D fixed point (see Sec. VI.B); whether larger scale separation can drive them into the 3D universality class remains an open question.

VII. CONCLUSION

The long-standing ultraviolet divergence paradox in the theory of non-thermal fixed points (NTFPs) has been resolved, and the first analytical prediction of a universal transport coefficient in far-from-equilibrium quantum dynamics is presented. While previous work focused solely on the scaling exponent $z = 2$, the prefactor C is determined explicitly. The geometric baseline $C = 3$ emerges from three ingredients: emergent weak U(1) symmetry forces diffusive phase dynamics with conserved noise; $z = 2$ scaling together with dynamical decoherence leads to a power-law momentum distribution $\tilde{f}(v) \sim (1+v^2)^{-3}$; and a marginally irrelevant coupling generates universal logarithmic corrections at finite scale separation. For the experimentally realized scale separation $\ell/\xi \approx 50$, these corrections quantitatively account for the measured value $C = 3.4(3)$ [31].

A new paradigm is thus established for predicting transport coefficients in strongly correlated non-equilibrium systems: symmetry constraints determine the low-energy effective theory, dynamical decoherence provides a natural ultraviolet completion via the power-law momentum distribution, and scaling analysis delivers parameter-free predictions for the geometric baseline together with a consistent explanation of logarithmic corrections. This paradigm moves beyond the determination of scaling exponents to the calculation of exact amplitudes. The power-law decay $\tilde{f}(v) \sim v^{-6}$ emerges as a generic dynamical regulator, suggesting that this decoherence mechanism may operate broadly across far-from-equilibrium systems.

Several open questions remain, including a first-principles derivation of the power-law distribution (equivalently the vortex correlation function with a lin-

ear prefactor) from the microscopic self-energy, and a direct microscopic calculation of the coefficients $D_\phi^{\rm macro}$ and A. Nevertheless, by demonstrating that quantitative predictions are possible without full microscopic control, the door is opened to precision studies of universality classes in quantum matter far from equilibrium. Together with parallel developments in fermionic systems [59], the present results indicate that irreducible correlations, whether from dynamical decoherence in bosons or collective modes in fermions, constitute a universal feature of quantum transport far from equilibrium.

We thank Huan Zhang, Ying Xia, Xiu-Xing Zhang, Zhen-Bin Zhang, and Jian-Ning Zhang for their encouragement, and Jie Wang and Ning Yue for valuable discussions. This research was supported by the Regional Collaborative Innovation Fund of Shanxi Province (Grant No. 2025QY-CY-YY05).

APPENDIX A: SYMMETRY AND MICROSCOPIC ORIGIN

This appendix provides the Keldysh field theory derivation of the modified Ward identity [Eq. (18)] used in Sec. III. The derivation employs the strong U(1) transformation (opposite phase rotations on the two contours) as a technical tool to incorporate dissipation into the symmetry constraints. The physical symmetry of the fixed point, however, is the exact weak U(1) symmetry (identical rotations), which guarantees total current conservation and underpins the low-energy Langevin theory presented in Appendix C.

1. Keldysh Field Theory Framework

The Keldysh closed-time path integral provides the fundamental framework for non-equilibrium quantum systems [6, 45–47]. The microscopic action in the Keldysh basis, Eq. (8) of the main text, is our starting point.

The classical field ψ_c and quantum field ψ_q have dimension $[L^{-3/2}]$, with $|\psi_c|^2$ giving particle density. Coefficients γ and $\tilde{D}$ (both $[T^{-1}]$) represent effective dissipation and noise from integrating out fast modes en route to the NTFP [17]. In our isolated system these are not external bath parameters but emerge from RG flow. The term $g|\psi_c|^2(\psi_c^*\psi_q + \text{c.c.})$ is the characteristic "ccq" vertex of the Keldysh technique for bosons. Dimensional consistency holds straightforwardly.

2. Rigorous Derivation of Modified Ward Identities

We now derive the modified Ward identities that encode how dissipation modifies the symmetry constraints at the NTFP.

2.1 Strong U(1) transformation

To derive the Ward identity for response to an external phase twist, we apply an infinitesimal local *strong U(1) transformation* with opposite phases on the two contours:

$$\psi_+(x) \to e^{i\theta(x)}\psi_+(x), \qquad \psi_-(x) \to e^{-i\theta(x)}\psi_-(x),$$

where $\theta(x)$ is spacetime-dependent. In the Keldysh basis $\psi_{c,q} = (\psi_+ \pm \psi_-)/\sqrt{2}$, this becomes

$$\begin{aligned} &\delta\psi_c = i\theta\,\psi_q, \quad \delta\psi_q = i\theta\,\psi_c, \\ &\delta\psi_c^* = -i\theta\,\psi_q^*, \quad \delta\psi_q^* = -i\theta\,\psi_c^*. \end{aligned} \tag{A1}$$

This choice preserves the causal structure of the Keldysh contour and is standard for response relations in open systems [6, 41, 46]. This strong U(1) transformation is a mathematical tool; it is not a symmetry of the dissipative action. The physical symmetry of the system is the weak U(1) transformation (identical phase rotations on both contours), which guarantees conservation of the total current as discussed in Appendix A3.

2.2 Variation of the action

The total action splits into a conserved part $S_{\rm cons}$ (kinetic and interaction terms) and a dissipative part $S_{\rm diss}$ [Eq. (8) of the main text]. We compute their variations separately.

We first consider the conserved part $S_{\rm cons}$. Under (A1), $S_{\rm cons}$ varies due to opposite contour rotations. The standard Noether procedure gives the divergence of the U(1) Noether current:

$$\delta S_{\rm cons} = \int_x \theta(x)\big[-\partial_t j^0(x) + \nabla\cdot\mathbf{j}(x)\big] + \mathcal{O}(\theta^2), \tag{A2}$$

with density and current

$$j^0 = \hbar|\psi_c|^2, \qquad \mathbf{j} = \frac{\hbar^2}{2mi}\big(\psi_c^*\nabla\psi_c - \psi_c\nabla\psi_c^*\big). \tag{A3}$$

A detailed derivation appears in Sec. 2.4 of Ref. [6].

We now turn to the dissipative part $S_{\rm diss}$. The dissipative action is

$$S_{\rm diss} = \int_x \big[i\hbar\gamma(\psi_q^*\psi_c + \psi_c^*\psi_q) + i\hbar\tilde{D}|\psi_q|^2\big]. \tag{A4}$$

Its functional derivatives are

$$\begin{aligned} &\frac{\delta S_{\rm diss}}{\delta\psi_c} = i\hbar\gamma\,\psi_q^*, \quad \frac{\delta S_{\rm diss}}{\delta\psi_c^*} = i\hbar\gamma\,\psi_q, \\ &\frac{\delta S_{\rm diss}}{\delta\psi_q} = i\hbar\gamma\,\psi_c^* + i\hbar\tilde{D}\,\psi_q^*, \quad \frac{\delta S_{\rm diss}}{\delta\psi_q^*} = i\hbar\gamma\,\psi_c + i\hbar\tilde{D}\,\psi_q. \end{aligned} \tag{A5}$$

Inserting the variations (A1) yields

$$\begin{aligned}\delta S_{\rm diss} &= \int_x \Big[(i\hbar\gamma\psi_q^*)(i\theta\psi_c) + (i\hbar\gamma\psi_q)(-i\theta\psi_c^*) \\ &\quad + (i\hbar\gamma\psi_c^* + i\hbar\tilde{D}\psi_q^*)(i\theta\psi_c) + (i\hbar\gamma\psi_c + i\hbar\tilde{D}\psi_q)(-i\theta\psi_c^*)\Big] \\ &= \int_x \Big[-\hbar\gamma\theta\,\psi_q^*\psi_c + \hbar\gamma\theta\,\psi_q\psi_c^* - \hbar\gamma\theta\,\psi_c^*\psi_c + \hbar\gamma\theta\,\psi_c\psi_c^* \\ &\quad - \hbar\tilde{D}\theta\,\psi_q^*\psi_c + \hbar\tilde{D}\theta\,\psi_q\psi_c^*\Big]. \end{aligned} \tag{A6}$$

Since ψ_c, ψ_q commute in the path integral, the terms $-\hbar\gamma\theta\,\psi_c^*\psi_c$ and $+\hbar\gamma\theta\,\psi_c\psi_c^*$ cancel exactly. The remaining four terms combine to

$$\delta S_{\rm diss} = -\hbar(\gamma+\tilde{D})\int_x \theta(x)\big(\psi_q^*\psi_c - \psi_c^*\psi_q\big). \tag{A7}$$

The combination $\psi_q^*\psi_c - \psi_c^*\psi_q = 2i\,\mathrm{Im}(\psi_q^*\psi_c)$ is purely imaginary and couples linearly to phase fluctuations. Both γ and $\tilde{D}$ appear, but at the NTFP they are linked by scale invariance, allowing combination into a single effective parameter.

2.3 Generating functional and exact Ward identity

The generating functional with sources J_c, J_q is

$$Z[J_c,J_q] = \int \mathcal{D}[\psi_c,\psi_q]\exp\Big[iS + i\int_x (J_c^*\psi_q + J_q^*\psi_c + \text{c.c.})\Big], \tag{A8}$$

with $\int_x \equiv \int dt\, d^3x$.

Invariance of the path-integral measure under (A1) gives

$$0 = \int \mathcal{D}[\psi_c,\psi_q]\, e^{iS + i\int(\cdots)}\Big[i\delta S + i\int_x \big(J_q^*\delta\psi_c + J_c^*\delta\psi_q + \text{c.c.}\big)\Big]. \tag{A9}$$

Substituting $\delta S = \delta S_{\rm cons} + \delta S_{\rm diss}$ and the explicit forms (A2) and (A7), and using that $\theta(x)$ is arbitrary, we obtain the exact operator identity (sources kept)

$$\begin{aligned} 0 &= \big\langle -\partial_t j^0(x) + \nabla\cdot\mathbf{j}(x)\big\rangle_J - \hbar(\gamma+\tilde{D})\big\langle\psi_q^*\psi_c - \psi_c^*\psi_q\big\rangle_J \\ &\quad + i\big[J_q^*(x)\langle\psi_c(x)\rangle_J + J_c^*(x)\langle\psi_q(x)\rangle_J - \text{c.c.}\big]. \end{aligned} \tag{A10}$$

2.4 Linear response and modified Ward identity

We seek retarded response functions in the absence of sources ($J_c, J_q \to 0$). Taking functional derivatives of Eq. (A10) with respect to J_q and J_q^* and then setting $J = 0$ yields relations among correlation functions. Fourier transforming to momentum k and frequency ω, and using the standard retarded response definition [46]

$$\chi^R_{AB}(\mathbf{k},\omega) = -i\int d^3r dt\, e^{-i\mathbf{k}\cdot\mathbf{r}+i\omega t}\Theta(t)\langle[A(\mathbf{r},t),B(0,0)]\rangle,$$

a standard Keldysh calculation (see Sec. 2.2 of Ref. [6]) gives the *modified Ward identity*

$$\begin{aligned}\omega\,\chi^R_{n\phi}(k,\omega) - \frac{\hbar n_0}{m}k^2\,\chi^R_{\phi\phi}(k,\omega) \\ = 2i(\gamma+\tilde{D})\,\chi^R_{\rm mix}(k,\omega) + \Delta_{\rm quantum},\end{aligned} \tag{A11}$$

where $n_0 = \langle|\psi_c|^2\rangle$ is the average density, and $\chi^R_{\rm mix}$ is a mixed response function involving $\mathrm{Im}(\psi_q^*\psi_c)$ and ϕ:

$$\begin{aligned}\chi^R_{\rm mix}(k,\omega) = -i\int d^3r dt\, e^{-i\mathbf{k}\cdot\mathbf{r}+i\omega t}\Theta(t) \\ \times\big\langle[\,\mathrm{Im}(\psi_q^*\psi_c)(\mathbf{r},t),\,\phi(0,0)\,]\big\rangle.\end{aligned} \tag{A12}$$

$\Delta_{\rm quantum}$ collects higher-order quantum correlations, negligible in the classical regime.

Equation (A11) is the exact consequence of strong U(1) symmetry with dissipation. The right-hand side is proportional to $\gamma+\tilde{D}$, showing both damping and noise modify the symmetry constraint.

2.5 Simplification at the NTFP

At the NTFP, the system exhibits emergent scale invariance and classicalization: occupation numbers become large ($n_k \gg 1$), suppressing quantum fluctuations [14, 17]. Thus $\Delta_{\rm quantum}$ can be dropped.

Scaling properties of the $z=2$ fixed point impose homogeneous scaling forms. In the long-wavelength limit, $\mathrm{Im}(\psi_q^*\psi_c)$ becomes dynamically conjugate to density fluctuations; kinetic-theory calculations at the NTFP [17] show that their response functions are proportional in the scaling regime,

$$\chi^R_{\rm mix}(k,\omega) \approx \beta_0\,\chi^R_{n\phi}(k,\omega) \qquad (k\to 0,\ \omega/k^2 \text{ fixed}), \tag{A13}$$

with β_0 a dimensionless constant of order unity. Physically, both operators are governed by the same low-energy phase fluctuations, collapsing onto a universal scaling function.

At the fixed point, the dissipation coefficient γ and noise coefficient $\tilde{D}$ are not independent; scale invariance implies that their ratio is a universal constant,

$$\frac{\tilde{D}}{\gamma} = \alpha_0, \tag{A14}$$

where α_0 is a dimensionless number determined by the fixed-point structure. (The explicit form of α_0 in terms of an effective temperature follows from an emergent fluctuation-dissipation-like relation at the NTFP (see Appendix C), which should be understood as an analog of, not a strict instance of, the equilibrium fluctuation-dissipation theorem.)

Inserting Eqs. (A13) and (A14) into (A11) and dropping Δ_{quantum} yields

$$\omega\chi^R_{n\phi} - \frac{\hbar n_0}{m}k^2\chi^R_{\phi\phi} = 2i\gamma(1+\alpha_0)\beta_0\,\chi^R_{n\phi}. \tag{A15}$$

Defining the effective dissipation coefficient $\gamma_{\text{eff}} \equiv \gamma(1+\alpha_0)\beta_0$, a universal constant at the NTFP, we obtain the working form used in the main text,

$$\omega\chi_{n\phi}(k,\omega) - \frac{\hbar n_0}{m}k^2\chi_{\phi\phi}(k,\omega) = 2i\gamma_{\text{eff}}\chi_{n\phi}(k,\omega), \tag{A16}$$

where the superscript R is dropped for simplicity. Equation (A16) breaks particle-number conservation yet retains the essential U(1) symmetry structure at the fixed point.

3. Weak U(1) Symmetry and Connection to Gauge-Invariant Response Theory

In the previous subsections we employed the strong U(1) transformation ($\psi_+ \to e^{i\theta}\psi_+$, $\psi_- \to e^{-i\theta}\psi_-$) as a technical tool to derive the modified Ward identity. That transformation is not a symmetry of the dissipative action, but its variation yields the exact identitie (A11). Here we instead focus on the weak U(1) symmetry ($\psi_\pm \to e^{i\theta}\psi_\pm$), which is an exact symmetry of our Keldysh action and provides the fundamental constraint that the total current (kinetic plus dissipative) is conserved, $\partial_\mu \bar{J}^\mu_c = 0$. This symmetry is precisely the one underlying the gauge-invariant response theory for open quantum systems developed by Li *et al.* [41].

Weak U(1) symmetry of the effective action. The Keldysh action we start from is given in Eq. (8). In the classical limit (high occupation numbers) characteristic of the NTFP, the fields ψ_c, ψ_q commute and the action can be written as

$$\begin{aligned} S = \int dt d^3x \Big[& \psi_q^*\big(i\hbar\partial_t + \tfrac{\hbar^2}{2m}\nabla^2\big)\psi_c + \text{c.c.} \\ & - \tfrac{g}{2}|\psi_c|^2(\psi_c^*\psi_q + \psi_q^*\psi_c) \\ & + i\hbar\gamma(\psi_q^*\psi_c + \psi_c^*\psi_q) + i\hbar\tilde{D}|\psi_q|^2\Big]. \end{aligned}$$

Under a *global* weak U(1) transformation

$$\psi_c \to e^{i\theta}\psi_c, \qquad \psi_q \to e^{i\theta}\psi_q,$$

each term in the action is manifestly invariant because every field appears together with its complex conjugate in a product, and the overall phase factors cancel. Consequently the action (and therefore the Lindbladian derived from it) satisfies the weak U(1) symmetry. Importantly, this symmetry does *not* require particle-number conservation; the dissipative terms $i\hbar\gamma(\psi_q^*\psi_c + \psi_c^*\psi_q)$ and $i\hbar\tilde{D}|\psi_q|^2$ are individually invariant, and they explicitly break particle number conservation at the microscopic level.

Consequences for the total current and noise. Applying the general result of Ref. [41] to our system, we can identify the kinetic part of the current with the usual supercurrent $J^\mu_c = \frac{\hbar^2}{2mi}(\psi_c^*\partial^\mu\psi_c - \partial^\mu\psi_c^*\psi_c)$ and the dissipative part J^μ_d as the contribution that arises from the terms γ and $\tilde{D}$ in the action. In the low-energy, long-wavelength limit, the total current conservation $\partial_\mu \bar{J}^\mu_c = 0$ imposes a constraint on the noise that enters the effective Langevin equation for the phase field. Specifically, the continuity equation $\partial_t n = -\nabla\cdot\bar{\mathbf{J}}_c$ together with the decomposition $\bar{\mathbf{J}}_c = -D^{\text{macro}}_\phi n_0\nabla\phi + \mathbf{J}_{\text{stoch}}$ yields the Langevin equation $\partial_t\phi = D^{\text{macro}}_\phi\nabla^2\phi + \zeta$ with $\zeta = -\nabla\cdot\mathbf{J}_{\text{stoch}}$. Assuming $\mathbf{J}_{\text{stoch}}$ is Gaussian white noise with $\langle J_i(\mathbf{r},t)J_j(\mathbf{r}',t')\rangle = \Gamma\delta_{ij}\delta(\mathbf{r}-\mathbf{r}')\delta(t-t')$, the noise correlation becomes $\langle\zeta(\mathbf{r},t)\zeta(\mathbf{r}',t')\rangle = -\Gamma\nabla^2\delta(\mathbf{r}-\mathbf{r}')\delta(t-t')$. Dimensional analysis and consistency with the macroscopic coarsening law $\ell^2(t) = 4D^{\text{macro}}_\phi t$ fix $\Gamma = 2D^{\text{macro}}_\phi\xi^3$, giving the conserved noise form used in Appendix C:

$$\langle\zeta(\mathbf{r},t)\zeta(\mathbf{r}',t')\rangle = -2D^{\text{macro}}_\phi\xi^3\,\nabla^2\delta(\mathbf{r}-\mathbf{r}')\delta(t-t').$$

Thus the symmetry-based construction of the noise correlation is not an ad hoc assumption but follows directly from the weak U(1) symmetry of the underlying Keldysh action.

Implications for the universal speed limit. This connection to the gauge-invariant response theory of Ref. [41] places our work on firm ground: the universal speed limit constant C is a consequence of symmetry-constrained transport in a system that, although dissipative and without particle-number conservation, still obeys the weak U(1) symmetry. The same symmetry guarantees that the total current is conserved, and therefore the diffusive growth law $\ell^2(t) = 4D^{\text{macro}}_\phi t$ derived in Appendix C is robust. Moreover, the explicit identification of the weak U(1) symmetry clarifies why the dissipative terms in our action do not spoil the Ward-Takahashi identity but instead modify it through the dissipative current J^μ_d, as already reflected in the modified Ward identity Eq. (A16). The essential role of weak U(1) symmetry in bounding quantum dynamics has also been demonstrated in the general proof of a universal speed limit on information scrambling by Ref. [12], where a regularized spectral form factor emerges from a similar symmetry-based mapping to non-unitary evolution.

APPENDIX B: PERTURBATIVE MECHANISM OF DISSIPATION GENERATION

To conceptually understand how interactions generate dissipative effects, we examine the phase field self-energy $\Sigma_{\phi\phi}$ within a perturbative framework. The NTFP is intrinsically a strong-coupling regime where the effective coupling scales as $g_{\text{eff}}(k) \sim k^2$ in the infrared [17].

In this perturbative analysis we treat g and γ_1 as constant parameters for illustration; it is **not intended** for quantitative predictions at the fixed point. Indeed, the calculation suffers from UV divergences and dimensional inconsistencies, signalling the need for a non-perturbative, symmetry-constrained treatment. Nevertheless, the analysis serves a valuable heuristic purpose: it demonstrates, in familiar diagrammatic language, that interactions naturally generate an imaginary (dissipative) component in the self-energy through the coupling of coherent modes (G^R) to background fluctuations (G^K). This progressive randomization of phase information via scattering is precisely the microscopic origin of the dynamical decoherence invoked in the main text. When consistently renormalized at the NTFP, this mechanism yields the Gaussian coherence weighting function $\mathcal{K}(v)$.

1. Perturbative analysis and its limitations

Dimensional analysis and the need for non-perturbative treatment We first establish the expected dimension of the phase-field self-energy $\Sigma^R_{\phi\phi}$. From the Dyson equation for the retarded response function,

$$\left[\chi^R_{\phi\phi}(k,\omega)\right]^{-1} = \left[\chi^R_{\phi\phi,0}(k,\omega)\right]^{-1} - \Sigma^R_{\phi\phi}(k,\omega), \qquad \text{(B1)}$$

where $\chi^R_{\phi\phi,0}$ is the bare response. Using the definition $\chi^R_{\phi\phi}(k,\omega) = -i\int d^3x dt\, e^{-i(\mathbf{k}\cdot\mathbf{x}-\omega t)}\langle[\phi(\mathbf{x},t),\phi(\mathbf{0},0)]\rangle\Theta(t)$, one finds $[\chi^R_{\phi\phi}] = [T]$ (since $[\phi] = 1$). Consequently, dimensional consistency of the Dyson equation requires $[\Sigma^R_{\phi\phi}] = [T^{-1}]$.

Now consider the one-loop contribution to the phase-field self-energy, depicted in Fig. 2:

$$\Sigma^R_{\phi\phi}(k,\omega) = -g^2 \int \frac{\mathrm{d}^3q}{(2\pi)^3}\frac{\mathrm{d}\Omega}{2\pi} G^K(q,\Omega)G^R(k-q,\omega-\Omega), \qquad \text{(B2)}$$

where the vertex factors $-ig$ originate from the $cc\phi$ interaction term in the Keldysh action. Using the dimensional assignments $[g] = ML^5T^{-2}$ (from $g = 4\pi\hbar^2 a/m$), $[\mathrm{d}^3q] = L^{-3}$, $[\mathrm{d}\Omega] = T^{-1}$, $[G^K] = [\langle\psi_c\psi_c^*\rangle] = L^{-3}$, and $[G^R] = [\chi^R_{\phi\phi}] = T$, the right-hand side has dimension

$$[g^2]\cdot[\mathrm{d}^3q]\cdot[\mathrm{d}\Omega]\cdot[G^K]\cdot[G^R] = M^2L^4T^{-4}, \qquad \text{(B3)}$$

which is manifestly inconsistent with the required $[T^{-1}]$. This discrepancy is not an error but a fundamental signature of the strong-coupling nature of the NTFP. Perturbation theory with constant bare parameters cannot capture the anomalous scaling dimensions characteristic of a scale-invariant fixed point. At the NTFP the effective coupling acquires a nontrivial momentum dependence $g_{\mathrm{eff}}(p) \sim p^2$ in the infrared [17], and the propagators develop corresponding scaling forms that restore dimensional consistency. The present calculation is therefore only qualitative. It serves to illustrate the mechanism by which interactions generate an imaginary (dissipative) component in the self-energy, not to provide quantitative predictions at the fixed point.

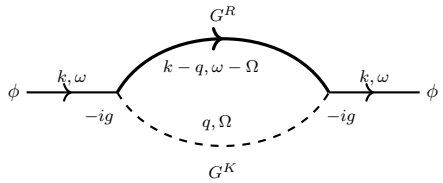

FIG. 2. One-loop Feynman diagram for the phase field self-energy $\Sigma^R_{\phi\phi}(k,\omega)$. The external field ϕ carries momentum (k,ω) and interacts at the vertices, generating internal propagators $G^R(k-q,\omega-\Omega)$ (solid line) and $G^K(q,\Omega)$ (dashed line). The vertex factors $-ig$ originate from the $cc\phi$ interaction term in the action. This diagram represents the coupling between coherent modes and background fluctuations that underlies decoherence. A full non-perturbative treatment is required for quantitative accuracy at the NTFP.

Physical interpretation The loop G^KG^R describes phase excitations scattering off the non-equilibrium background. The retarded propagator G^R captures coherent propagation, while the Keldysh propagator G^K incorporates the inherent noise of the driven-dissipative environment. Physically, each scattering event transfers coherence information into dissipative channels, progressively randomizing the phase. The cumulative effect appears as an imaginary component in the self-energy, which underlies the dynamical decoherence mechanism central to resolving the UV divergence paradox. This qualitative picture remains valid even though a full non-perturbative treatment is required for quantitative accuracy.

2. Physical interpretation and self-energy scaling at the NTFP

The perturbative analysis above reveals the fundamental mechanism by which interactions generate dissipation. The product G^KG^R in the self-energy represents energy transfer from collective modes to the non-equilibrium excitation "bath": G^K encodes the noise of the background, while G^R describes coherent propagation. Each scattering event randomizes phase information, and the cumulative effect appears as an imaginary component in $\Sigma^R_{\phi\phi}$, representing the microscopic origin of the dynamical decoherence mechanism invoked in the main text.

This analysis also highlights why a non-perturbative treatment is essential. A direct one-loop evaluation yields a linearly divergent self-energy and violates dimensional consistency, which would imply a mass for the phase mode and contradict the Goldstone theorem, confirm-

ing that naive perturbation theory fails at the NTFP. At the true NTFP, these issues are resolved by the universal scaling of the effective coupling: $g_{\rm eff}(p) \sim p^2$ in the infrared [17]. This momentum dependence restores dimensional consistency, ensures $\Sigma^R_{\phi\phi} \sim k^2$ as $k \to 0$, and renders physical observables like D_ϕ UV-convergent. The full symmetry-constrained analysis, which does not rely on perturbative expansion, is presented in Appendix C.

The above perturbative analysis used constant coupling g and constant damping γ_1, which are not adequate for the strongly correlated NTFP. However, the qualitative lesson that interactions generate an imaginary self-energy remains valid. At the NTFP, the effective coupling acquires a momentum-dependent scaling $g_{\rm eff}(p) \sim g_0(p\xi)^2$ in the infrared, while the propagators follow the scaling forms characteristic of the $z = 2$ fixed point [17]. With these inputs, a one-loop calculation analogous to Eq. (B2) becomes UV convergent. The resulting retarded self-energy satisfies

$$\mathrm{Im}\,\Sigma^R_{\phi\phi}(k,\omega) \sim D_\phi k^2 \qquad (k \to 0),$$

as can be inferred from the scaling analysis of Ref. [17] together with the symmetry constraints discussed in Appendix C. This scaling behavior is precisely what is needed to realize the diffusive pole and, as discussed in Sec. IV, underlies the dynamical decoherence that resolves the ultraviolet divergence. Thus the microscopic dissipation mechanism discussed here, when consistently renormalized at the NTFP, leads to the universal decoherence effect that regularizes the UV contribution and yields a convergent moment ratio. This mechanism is directly visualized in the vortex imaging experiment of Ref. [50], where the random vortex tangle corresponds to the imaginary self-energy.

APPENDIX C: MACROSCOPIC COARSENING DYNAMICS AND UNIVERSAL CONSTANT DERIVATION

This appendix derives the macroscopic consequences of the symmetry-constrained diffusive dynamics established in Secs. III.B and III.C. Starting from the effective Langevin equation enforced by emergent weak U(1) symmetry at the NTFP, we obtain the conserved noise correlation, the diffusive growth law $\ell^2(t) = 4D_\phi^{\rm macro} t$, and the central relation $C = 4mD_\phi^{\rm macro}/\hbar$. The macroscopic coefficient $D_\phi^{\rm macro}$ is defined in Eq. (30) and related to the microscopic diffusion coefficient via $D_\phi^{\rm macro} = D_\phi/(n\xi^3)$; the scaling origin of this relation is discussed in Sec. III.C. The following subsections provide detailed derivations underlying the results presented in Sec. III.D of the main text.

1. Effective Langevin Equation and Conserved Noise from Symmetry and Scaling

The effective Langevin equation (31) and the conserved noise correlation (32) can be derived from the Keldysh action (8) by separating slow condensate and fast quasiparticle modes and integrating out the latter [46]. In the classical-wave limit characteristic of the NTFP [17], this yields an effective action for the condensate alone. For a closed system with exact U(1) symmetry, the noise enters as the divergence of a conserved current, giving the $\nabla^2\delta$ correlation structure. Moreover, at the $z = 2$ fixed point, the effective many-body coupling scales as $g_{\rm eff}(p) \sim p^2$ [17], which leads to the diffusive phase self-energy derived in Sec. III.B.

A full first-principles derivation requires non-perturbative techniques beyond our scope. Instead, we construct the effective Langevin equation directly from symmetry, scaling, and dimensional analysis. Weak U(1) symmetry forces the noise to appear as the divergence of a conserved current; $z = 2$ scaling fixes the derivative order; and dimensional consistency determines the amplitude in terms of $D_\phi^{\rm macro}$ and ξ. This yields the unique low-energy effective theory consistent with the NTFP, whose validity is ultimately justified by quantitative agreement with experiment (see main text). This symmetry-based construction is analogous to the approach recently developed for phase separation in binary Bose superfluids [39].

Noise as divergence of a stochastic current. In a microscopic derivation, integrating out fast modes typically produces a noise that is local in space and time, $\langle\zeta(\mathbf{r},t)\zeta(\mathbf{r}',t')\rangle \propto \delta(\mathbf{r}-\mathbf{r}')\delta(t-t')$. However, to respect the exact U(1) symmetry of the closed system, the noise must instead enter as the divergence of a conserved current; this transforms its correlation into the $\nabla^2\delta$ form. This construction is placed on firm microscopic ground by the weak U(1) symmetry of the Keldysh action (see Appendix A3), which guarantees total current conservation. Particle number conservation requires that any stochastic forcing of the phase field must couple through the divergence of a stochastic current. The most general form of noise consistent with emergent U(1) symmetry and spatial locality is

$$\zeta(\mathbf{r},t) = \nabla\cdot\mathbf{J}(\mathbf{r},t), \tag{C1}$$

where $\mathbf{J}(\mathbf{r},t)$ is a stochastic current. This form automatically satisfies $\int d^3r\,\zeta(\mathbf{r},t) = 0$ (assuming vanishing boundary terms), ensuring global symmetry preservation [60].

To obtain a closed Langevin equation, we adopt the standard assumption that $\mathbf{J}$ is Gaussian white noise. The final results depend only on the second moment of $\mathbf{J}$ and are therefore independent of the Gaussian approxima-

tion. With this assumption,

$$\langle J_i(\mathbf{r},t)J_j(\mathbf{r}',t')\rangle = \Gamma\,\delta_{ij}\,\delta^{(3)}(\mathbf{r}-\mathbf{r}')\delta(t-t'), \tag{C2}$$

where $\Gamma > 0$ is the noise intensity. Combining Eqs. (C1) and (C2) yields

$$\langle \zeta(\mathbf{r},t)\zeta(\mathbf{r}',t')\rangle = \Gamma\,\nabla^2\delta^{(3)}(\mathbf{r}-\mathbf{r}')\delta(t-t'). \tag{C3}$$

Determining the noise intensity. The noise intensity Γ is fixed by the scaling properties of the NTFP. Dimensional analysis and the requirement that the noise correlation respects $z = 2$ scale invariance lead to the unique form

$$\Gamma = 2D_\phi^{\rm macro}\xi^3, \tag{C4}$$

where $D_\phi^{\rm macro}$ is the macroscopic phase diffusion coefficient defined in Eq. (30) and ξ is the healing length. Substituting into Eq. (C3) gives the conserved noise correlation in terms of macroscopic quantities

$$\langle \zeta(\mathbf{r},t)\zeta(\mathbf{r}',t')\rangle = -2D_\phi^{\rm macro}\xi^3\,\nabla^2\delta^{(3)}(\mathbf{r}-\mathbf{r}')\delta(t-t'), \tag{C5}$$

where the minus sign ensures positive-definiteness in Fourier space (since $\nabla^2 \to -k^2$). This form respects the emergent U(1) symmetry and is consistent with the scaling dimensions at the $z = 2$ fixed point [14, 60]. Both sides have dimension $[T^{-2}]$, confirming dimensional consistency. The resulting conserved noise correlation provides the essential input for the dimensionless analysis that follows (Secs. 2–6).

Emergent fluctuation-dissipation relation and effective temperature. As discussed in Sec. III.C, the NTFP exhibits an emergent fluctuation-dissipation relation characterized by an effective temperature $T_{\rm eff}$. To quantify the quantum pressure scale that sets the noise amplitude, we directly define

$$T_{\rm eff} = \frac{\hbar^2 n^{2/3}}{m k_B}. \tag{C6}$$

This choice is natural because $\hbar^2 n^{2/3}/m$ has dimension of energy and captures the kinetic energy scale associated with the average interparticle spacing $n^{-1/3}$. For a weakly interacting Bose gas at the NTFP, the healing length $\xi = \hbar/\sqrt{2mgn}$ gives an alternative energy scale $gn = \hbar^2/(2m\xi^2)$. These two scales are generally different (their ratio is $4\pi a n^{1/3}$ in three dimensions), and we adopt the $n^{2/3}$ form because it remains constant during scaling evolution (since the total density n is fixed) and properly reflects the quantum pressure that underlies phase fluctuations. The scaling $T_{\rm eff} \propto n^{2/3}$ is consistent with the fixed-point structure.

Although $T_{\rm eff}$ does not appear explicitly in the final noise correlation (C5), it provides the physical interpretation of the fluctuation scale and ensures consistency with the emergent thermodynamic structure described in the main text.

The noise correlation function (C5) is not derived from first principles by integrating out microscopic degrees of freedom, a task intractable at the strong-coupling NTFP. Instead, it is constructed as the most general form consistent with emergent U(1) symmetry, $z = 2$ scale invariance, and dimensional analysis. The coefficient $2D_\phi^{\rm macro}\xi^3$ is uniquely fixed by requiring that the resulting Langevin equation reproduces the correct diffusive growth law $\ell^2 = 4D_\phi^{\rm macro}t$ and aligns with the fluctuation-dissipation structure encoded in $T_{\rm eff}$. This constructive approach, standard in effective field theories of far-from-equilibrium critical phenomena, provides a robust foundation for the subsequent derivation of coherence growth laws. The conserved form $\langle\zeta\zeta\rangle \propto -\nabla^2\delta\delta$ is precisely the structure required to generate diffusive phase spreading while respecting particle number conservation [60]. The ultimate justification lies in its quantitative agreement with experiment (see main text).

2. Dimensionless Framework and Scale Invariance at the NTFP

At the NTFP, the system exhibits emergent scale invariance with dynamic critical exponent $z = 2$. To ensure dimensional consistency and exploit the scale invariance, we introduce a dimensionless framework using characteristic scales of the system. The natural characteristic length is the healing length $\xi = \hbar/\sqrt{2mgn}$, which sets the scale for density variations [43, 44]. The corresponding characteristic time is the free-particle diffusion time across a healing length, $\tau_0 = m\xi^2/\hbar$. In addition, we define a dimensionless phase diffusion coefficient $\tilde{D}_\phi \equiv mD_\phi^{\rm macro}/\hbar$, where $D_\phi^{\rm macro}$ is the macroscopic phase diffusion coefficient defined in Eq. (30); at the NTFP $\tilde{D}_\phi$ becomes a universal constant, independent of microscopic details.

Dimensionless variables are then introduced as

$$\tilde{\mathbf{r}} = \frac{\mathbf{r}}{\xi}, \quad \tilde{t} = \frac{t}{\tau_0} = \frac{\hbar t}{m\xi^2}, \tag{C7}$$

$$\tilde{\phi}(\tilde{\mathbf{r}},\tilde{t}) = \phi(\mathbf{r},t), \quad \tilde{\zeta}(\tilde{\mathbf{r}},\tilde{t}) = \tau_0\zeta(\mathbf{r},t). \tag{C8}$$

In these dimensionless units, the Langevin equation for the phase field takes the simple form

$$\frac{\partial\tilde{\phi}}{\partial\tilde{t}} = \tilde{D}_\phi\tilde{\nabla}^2\tilde{\phi} + \tilde{\zeta}(\tilde{\mathbf{r}},\tilde{t}), \tag{C9}$$

where $\tilde{\nabla}$ denotes the gradient with respect to the dimensionless coordinate $\tilde{\mathbf{r}}$.

3. Construction of Dimensionless Noise Correlation Function

The dimensional noise correlation function in Eq. (C5) transforms into dimensionless form as follows. Using the definitions in Eq. (C8) and the relation $\tilde{D}_\phi = mD_\phi^{\rm macro}/\hbar = mD_\phi/(\hbar n\xi^3)$, we obtain

$$\langle\tilde{\zeta}(\tilde{\mathbf{r}},\tilde{t})\tilde{\zeta}(\tilde{\mathbf{r}}',\tilde{t}')\rangle = -2\tilde{D}_\phi\tilde{\nabla}^2\delta(\tilde{\mathbf{r}}-\tilde{\mathbf{r}}')\delta(\tilde{t}-\tilde{t}'). \quad \text{(C10)}$$

This conserved form, with the Laplacian operator, ensures that noise enters as a divergence of a conserved current, consistent with the approximate particle number conservation. The factor $-2\tilde{D}_\phi$ is consistent with the effective temperature $T_{\rm eff}$ defined in Sec. 1 and with the scaling properties of the NTFP.

In the dimensionless framework all quantities are dimensionless by construction: $\tilde{\zeta} = \tau_0\zeta$ is dimensionless by definition; $\tilde{D}_\phi = mD_\phi^{\rm macro}/\hbar$ is likewise dimensionless; the Laplacian $\tilde{\nabla}^2$ involves derivatives with respect to $\tilde{\mathbf{r}} = \mathbf{r}/\xi$ and is therefore dimensionless; and the Dirac delta functions $\delta(\tilde{\mathbf{r}})$ and $\delta(\tilde{t})$ are also dimensionless because they are taken with respect to dimensionless coordinates. Consequently both sides of Eq. (C10) are manifestly dimensionless, ensuring dimensional consistency in the dimensionless framework.

4. Coherence Length Growth in Dimensionless Units

Before performing the explicit calculation, we note that dimensional analysis and scaling alone determine the growth law up to a dimensionless constant: $\ell^2(t) \propto D_\phi^{\rm macro}t$. To fix the numerical coefficient, we adopt the standard Gaussian white noise approximation for the stochastic current, which yields a tractable Langevin equation. The resulting coefficient is a convention: we define $D_\phi^{\rm macro}$ precisely so that $\ell^2 = 4D_\phi^{\rm macro}t$. This choice does not rely on the Gaussian assumption; any other definition would merely rescale $D_\phi^{\rm macro}$ and leave the physical observable C unchanged, as will become clear in the relation $C = 4mD_\phi^{\rm macro}/\hbar$ (see Sec. 5 below). The following derivation follows this approach.

In dimensionless units, the diffusion Green's function satisfying $\partial\tilde{G}/\partial\tilde{t} = \tilde{D}_\phi\tilde{\nabla}^2\tilde{G} + \delta(\tilde{\mathbf{r}})\delta(\tilde{t})$ is

$$\tilde{G}(\tilde{\mathbf{r}},\tilde{t}) = \frac{1}{(4\pi\tilde{D}_\phi\tilde{t})^{3/2}}\exp\left(-\frac{\tilde{r}^2}{4\tilde{D}_\phi\tilde{t}}\right). \quad \text{(C11)}$$

The formal solution for the phase field is

$$\tilde{\phi}(\tilde{\mathbf{r}},\tilde{t}) = \int_0^{\tilde{t}} d\tilde{t}' \int d^3\tilde{r}'\tilde{G}(\tilde{\mathbf{r}}-\tilde{\mathbf{r}}',\tilde{t}-\tilde{t}')\tilde{\zeta}(\tilde{\mathbf{r}}',\tilde{t}'). \quad \text{(C12)}$$

The phase difference variance follows from substituting the noise correlation (C10)

$$\langle[\tilde{\phi}(\tilde{\mathbf{r}},\tilde{t}) - \tilde{\phi}(0,\tilde{t})]^2\rangle = \int_0^{\tilde{t}} d\tilde{t}_1 \int_0^{\tilde{t}} d\tilde{t}_2 \int d^3\tilde{r}_1 d^3\tilde{r}_2 \times [\tilde{G}(\tilde{\mathbf{r}}-\tilde{\mathbf{r}}_1,\tilde{t}-\tilde{t}_1) - \tilde{G}(-\tilde{\mathbf{r}}_1,\tilde{t}-\tilde{t}_1)] \times [\tilde{G}(\tilde{\mathbf{r}}-\tilde{\mathbf{r}}_2,\tilde{t}-\tilde{t}_2) - \tilde{G}(-\tilde{\mathbf{r}}_2,\tilde{t}-\tilde{t}_2)]\langle\tilde{\zeta}(\tilde{\mathbf{r}}_1,\tilde{t}_1)\tilde{\zeta}(\tilde{\mathbf{r}}_2,\tilde{t}_2)\rangle. \quad \text{(C13)}$$

After integration by parts (transferring $\tilde{\nabla}^2$ to act on the Green's functions) and using $\tilde{\nabla}\tilde{G}(\tilde{\mathbf{r}},\tilde{t}) = -\frac{\tilde{\mathbf{r}}}{2\tilde{D}_\phi\tilde{t}}\tilde{G}(\tilde{\mathbf{r}},\tilde{t})$, we obtain in the long-time limit ($\tilde{t} \gg \tilde{r}^2/\tilde{D}_\phi$)

$$\langle[\tilde{\phi}(\tilde{\mathbf{r}},\tilde{t}) - \tilde{\phi}(0,\tilde{t})]^2\rangle \approx \frac{\tilde{r}^2}{2\tilde{D}_\phi\tilde{t}}\cdot\mathcal{F}\left(\frac{\tilde{r}}{\sqrt{\tilde{D}_\phi\tilde{t}}}\right), \quad \text{(C14)}$$

with the scaling function $\mathcal{F}(x) \to 1$ for $x \ll 1$. Thus for $\tilde{r} \ll \sqrt{\tilde{D}_\phi\tilde{t}}$ we obtain

$$\langle[\tilde{\phi}(\tilde{\mathbf{r}},\tilde{t}) - \tilde{\phi}(0,\tilde{t})]^2\rangle \approx \frac{\tilde{r}^2}{2\tilde{D}_\phi\tilde{t}}. \quad \text{(C15)}$$

The dimensionless coherence length $\tilde{\ell}(\tilde{t})$ is defined by the condition that the phase correlation function decays to $1/e$, which for Gaussian fluctuations corresponds to

$$\langle[\tilde{\phi}(\tilde{\ell}(\tilde{t}),\tilde{t}) - \tilde{\phi}(0,\tilde{t})]^2\rangle = 2. \quad \text{(C16)}$$

Substituting Eq. (C15) with $\tilde{r} = \tilde{\ell}(\tilde{t})$ yields the fundamental growth law in dimensionless form

$$\frac{\tilde{\ell}^2(\tilde{t})}{2\tilde{D}_\phi\tilde{t}} = 2 \quad \Rightarrow \quad \tilde{\ell}^2(\tilde{t}) = 4\tilde{D}_\phi\tilde{t}. \quad \text{(C17)}$$

The coefficient 4 is thus a direct consequence of the chosen definition of $D_\phi^{\rm macro}$ (via $\ell^2 = 4D_\phi^{\rm macro}t$). As emphasized above, this definition is a convention that does not rely on the Gaussian approximation; it merely sets the scale for $D_\phi^{\rm macro}$. The physical quantity $C = 4mD_\phi^{\rm macro}/\hbar$ (derived in Sec. 5 below) is independent of this convention because any rescaling of $D_\phi^{\rm macro}$ would be compensated by the experimental determination of C.

5. Equivalence of Theoretical and Experimental Coherence Length Definitions

A crucial step in connecting our theoretical framework to experiment is to demonstrate that the coherence length $\ell(t)$ extracted from the momentum distribution in the experiment [31] is identical to the theoretical coherence length governing phase correlations. This equivalence relies on two assumptions, validated in the scaling regime of the NTFP: (1) negligible density fluctuations

$\delta n \ll n$, and (2) spatial homogeneity at scales larger than the healing length ξ. (The Gaussian statistics often invoked for simplicity is not required for the equivalence itself, as shown below.)

We begin by stating the two independent definitions. Theoretically, the coherence length is defined by the decay of the phase correlation function

$$C_\phi(\ell(t),t) \equiv \langle e^{i[\phi(\mathbf{r},t)-\phi(\mathbf{0},t)]}\rangle\Big|_{r=\ell(t)} = e^{-1}. \tag{C18}$$

Experimentally, it is extracted from the scaling form of the momentum distribution [31]

$$n_k(\mathbf{k},t) = \ell^3(t) f(k\ell(t)), \tag{C19}$$

where $f(v)$ is a universal scaling function and $v = k\ell(t)$.

To connect the two definitions, we consider the first-order correlation function $g^{(1)}(\mathbf{r},t) = \langle\hat{\Psi}^\dagger(\mathbf{r},t)\hat{\Psi}(\mathbf{0},t)\rangle$. In the hydrodynamic description, $\hat{\Psi}(\mathbf{r},t) = \sqrt{n(\mathbf{r},t)}e^{i\phi(\mathbf{r},t)}$. Under assumption (1) of constant density, $n(\mathbf{r},t)\approx n$, this becomes

$$g^{(1)}(\mathbf{r},t) \approx n\langle e^{i[\phi(\mathbf{0},t)-\phi(\mathbf{r},t)]}\rangle = nC_\phi(\mathbf{r},t). \tag{C20}$$

The momentum distribution is the Fourier transform of $g^{(1)}$:

$$n_k(\mathbf{k},t) = \int d^3r\, e^{-i\mathbf{k}\cdot\mathbf{r}} g^{(1)}(\mathbf{r},t) = n\int d^3r\, e^{-i\mathbf{k}\cdot\mathbf{r}} C_\phi(\mathbf{r},t). \tag{C21}$$

Now we use the dynamic scaling property of the NTFP, which follows from the $z=2$ fixed point (see Sec. III.B): the phase correlation function depends only on the ratio $r/\ell(t)$, i.e., $C_\phi(\mathbf{r},t) = F(r/\ell(t))$ with $F(1) = e^{-1}$ by the theoretical definition. Substituting this scaling form into Eq. (C21) and changing variables $\mathbf{u} = \mathbf{r}/\ell(t)$, $\mathbf{v} = \mathbf{k}\ell(t)$ yields

$$n_k(\mathbf{k},t) = n\ell^3(t)\int d^3u\, e^{-i\mathbf{v}\cdot\mathbf{u}} F(u). \tag{C22}$$

The integral is a function of $v = |\mathbf{v}|$ only and is independent of t because F is fixed. Thus we have

$$n_k(\mathbf{k},t) = n\ell^3(t)\,\tilde{f}(k\ell(t)), \tag{C23}$$

where $\tilde{f}(v) = \int d^3u\, e^{-i\mathbf{v}\cdot\mathbf{u}}F(u)$ is a universal function. This establishes the scaling form of Eq. (C19) with $f(v) = n\tilde{f}(v)$. Moreover, the theoretical definition $C_\phi(\ell) = e^{-1}$ fixes the normalization of F and therefore does not affect the scaling form; it merely sets the scale of $\ell(t)$.

Hence, the length scale $\ell(t)$ appearing in the experimental momentum distribution is precisely the same coherence length defined by the decay of phase correlations. The derivation above does **not** require the assumption of Gaussian statistics; it only uses the scaling property of C_ϕ and the definition of $\ell(t)$.

Having established the equivalence, we now relate the coherence growth to the macroscopic phase diffusion coefficient. From the symmetry and scaling analysis of Sec. III and this appendix, the low-energy phase dynamics is diffusive, implying $\ell^2(t) \propto D_\phi^{\rm macro} t$. The numerical coefficient is fixed by a convention: we define $D_\phi^{\rm macro}$ such that

$$\ell^2(t) = 4D_\phi^{\rm macro} t, \tag{C24}$$

as discussed in Secs. 4 and 6. This definition is independent of any specific model for the fluctuations; any other prefactor would merely rescale $D_\phi^{\rm macro}$ and leave the physically observable C invariant. Finally, comparing Eq. (C24) with the experimental relation $d\ell^2/dt = C\hbar/m$ gives the central connection

$$C = \frac{4mD_\phi^{\rm macro}}{\hbar}. \tag{C25}$$

In summary, this equivalence proof validates our framework by showing that the microscopic phase dynamics we analyze give rise to the same coherence length observed experimentally, thereby enabling a quantitative calculation of C. This universal behavior is intimately related to the concept of hydrodynamic attractors [55] and arises whenever multi-particle scattering destroys integrability constraints [54].

Remark. If one additionally assumes Gaussian statistics for the phase fluctuations (a common but non-essential simplification), the phase correlation function takes the explicit form $C_\phi(r,t) = \exp(-r^2/\ell^2(t))$, and the diffusion equation gives $\langle[\phi(r,t)-\phi(0,t)]^2\rangle = 2r^2/\ell^2(t)$. These specific forms are consistent with the general scaling analysis and the definitions above, but they are not required for the equivalence proof or for the final relation $C = 4mD_\phi^{\rm macro}/\hbar$.

6. Physical Synthesis

The dimensionless framework establishes a self-consistent theoretical chain: symmetry principles yield conserved noise; the Langevin equation gives diffusive coherence growth $\ell^2 = 4D_\phi^{\rm macro}t$; and the relation $C = 4mD_\phi^{\rm macro}/\hbar$ connects microscopic transport to the universal constant. Crucially, the derivation involves no adjustable parameters, only universal fixed-point properties and the coherence length definition. The vortex imaging experiment of Ref. [50] provides direct microscopic support for this construction: the random, divergence-free vortex tangle gives a concrete realization of the conserved noise assumed in the Langevin equation, and the observed $1/t$ decay of the vortex line-length density independently implies $\ell^2 \propto t$ via $\ell \sim$ vortex spacing, confirming the diffusive growth law.

Note on the coefficient 4. The coefficient 4 in $\ell^2 = 4D_\phi^{\rm macro}t$ is a convention that defines $D_\phi^{\rm macro}$; it does not

rely on the Gaussian approximation and does not affect the final prediction for C. The relation $C = 4mD_\phi^{\rm macro}/\hbar$ is a definitional consequence of the experimental growth law $d\ell^2/dt = C\hbar/m$ and the definition of $D_\phi^{\rm macro}$, and holds regardless of the statistical nature of the phase fluctuations.

* liangjuncheng@wnu.edu.cn

[1] A. Polkovnikov, K. Sengupta, A. Silva, and M. Vengalattore, Colloquium: Nonequilibrium dynamics of closed interacting quantum systems, Rev. Mod. Phys. **83**, 863 (2011).

[2] J. Berges, M. P. Heller, A. Mazeliauskas, and R. Venugopalan, Qcd thermalization: Ab initio approaches and interdisciplinary connections, Rev. Mod. Phys. **93**, 035003 (2021).

[3] J. Eisert, M. Friesdorf, and C. Gogolin, Quantum many-body systems out of equilibrium, Nat. Phys. **11**, 124 (2015).

[4] L. W. Clark, L. Feng, and C. Chin, Universal space-time scaling symmetry in the dynamics of bosons across a quantum phase transition, Science **354**, 606 (2016).

[5] U. Eismann, L. Khaykovich, S. Laurent, I. Ferrier-Barbut, B. S. Rem, A. T. Grier, M. Delehaye, F. Chevy, C. Salomon, L.-C. Ha, and C. Chin, Universal loss dynamics in a unitary bose gas, Phys. Rev. X **6**, 021025 (2016).

[6] L. M. Sieberer, M. Buchhold, and S. Diehl, Keldysh field theory for driven open quantum systems, Rep. Prog. Phys. **79**, 096001 (2016).

[7] C. Gao, M. Sun, P. Zhang, and H. Zhai, Universal dynamics of a degenerate bose gas quenched to unitarity, Phys. Rev. Lett. **124**, 040403 (2020).

[8] Z.-Y. Shi, C. Gao, and H. Zhai, Ideal-gas approach to hydrodynamics, Phys. Rev. X **11**, 041031 (2021).

[9] N. P. Proukakis, Universality of Bose–Einstein condensation and quenched formation dynamics, in *Encyclopedia of Condensed Matter Physics (Second Edition)*, edited by T. Chakraborty (Academic Press, Oxford, 2024) second edition ed., pp. 84–123.

[10] Y. Li, T.-G. Zhou, Z. Wu, P. Peng, S. Zhang, R. Fu, R. Zhang, W. Zheng, P. Zhang, H. Zhai, X. Peng, and J. Du, Emergent universal quench dynamics in randomly interacting spin models, Nat. Phys. **20**, 1966 (2024).

[11] T. Zhang, H. Wang, W. Zhang, Y. Wang, A. Du, Z. Li, Y. Wu, C. Li, J. Hu, H. Zhai, and W. Chen, Observation of near-critical kibble-zurek scaling in rydberg atom arrays, Phys. Rev. Lett. **135**, 093403 (2025).

[12] A. Vikram, L. Shou, and V. Galitski, Proof of a universal speed limit on fast scrambling in quantum systems, Phys. Rev. Lett. **136**, 150401 (2026).

[13] E. H. Lieb and D. W. Robinson, The finite group velocity of quantum spin systems, Commun. Math. Phys. **28**, 251 (1972).

[14] J. Berges, A. Rothkopf, and J. Schmidt, Nonthermal fixed points: Effective weak coupling for strongly correlated systems far from equilibrium, Phys. Rev. Lett. **101**, 041603 (2008).

[15] B. Nowak, J. Schole, D. Sexty, and T. Gasenzer, Nonthermal fixed points, vortex statistics, and superfluid turbulence in an ultracold Bose gas, Phys. Rev. A **85**, 043627 (2012).

[16] A. Piñeiro Orioli, K. Boguslavski, and J. Berges, Universal self-similar dynamics of relativistic and nonrelativistic field theories near nonthermal fixed points, Phys. Rev. D **92**, 025041 (2015).

[17] I. Chantesana, A. Piñeiro Orioli, and T. Gasenzer, Kinetic theory of nonthermal fixed points in a Bose gas, Phys. Rev. A **99**, 043620 (2019).

[18] T. W. B. Kibble, Topology of cosmic domains and strings, J. Phys. A **9**, 1387 (1976).

[19] B. V. Svistunov, Superfluid turbulence in the low-temperature limit, Phys. Rev. B **52**, 3647 (1995).

[20] W. F. Vinen and J. J. Niemela, Quantum turbulence, J. Low Temp. Phys. **128**, 167 (2002).

[21] M. Gazo, A. Karailiev, T. Satoor, C. Eigen, M. Gałka, and Z. Hadzibabic, Universal coarsening in a homogeneous two-dimensional Bose gas, Science **389**, 802 (2025).

[22] S. P. Johnstone, A. J. Groszek, P. T. Starkey, C. J. Billington, T. P. Simula, and K. Helmerson, Evolution of large-scale flow from turbulence in a two-dimensional superfluid, Science **364**, 1267 (2019).

[23] M. Prüfer *et al.*, Observation of universal dynamics in a spinor Bose gas far from equilibrium, Nature **563**, 217 (2018).

[24] S. Huh *et al.*, Universality class of a spinor Bose-Einstein condensate far from equilibrium, Nat. Phys. **20**, 402 (2024).

[25] J. A. P. Glidden *et al.*, Bidirectional dynamic scaling in an isolated Bose gas far from equilibrium, Nat. Phys. **17**, 457 (2021).

[26] A. D. García-Orozco, L. Madeira, M. A. Moreno-Armijos, A. R. Fritsch, P. E. S. Tavares, P. C. M. Castilho, A. Cidrim, G. Roati, and V. S. Bagnato, Universal dynamics of a turbulent superfluid Bose gas, Phys. Rev. A **106**, 023314 (2022).

[27] S. Erne, R. Bücker, T. Gasenzer, J. Berges, and J. Schmiedmayer, Universal dynamics in an isolated one-dimensional Bose gas far from equilibrium, Nature **563**, 225 (2018).

[28] Q. Liang, R. Wu, P. Paranjape, B. Schittenkopf, C. Li, J. Schmiedmayer, and S. Erne, Universal non-thermal fixed point for quasi-1d Bose gases, arXiv preprint arXiv:2505.20213 (2025), see also the experimental crossover scaling analysis therein.

[29] L. Madeira and V. S. Bagnato, Non-thermal fixed points in Bose gas experiments, Symmetry **14**, 10.3390/sym14040678 (2022).

[30] A. N. Mikheev, I. Siovitz, and T. Gasenzer, Universal dynamics and non-thermal fixed points in quantum fluids far from equilibrium, Eur. Phys. J. Spec. Top. **232**, 3393 (2023).

[31] G. Martirosyan, M. Gazo, J. Etrych, S. M. Fischer, S. J. Morris, C. J. Ho, C. Eigen, and Z. Hadzibabic, A universal speed limit for spreading of coherence, Nature **647**, 608 (2025).

[32] C.-F. A. Chen, A. Lucas, and C. Yin, Speed limits and locality in many-body quantum dynamics, Rep. Prog. Phys. **86**, 116001 (2023).

[33] P. M. Chaikin and T. C. Lubensky, *Principles of Condensed Matter Physics* (Cambridge University Press, 1995).

[34] H. T. C. Stoof, Formation of the condensate in a dilute Bose gas, Phys. Rev. Lett. **66**, 3148 (1991).

[35] B. V. Svistunov, Highly nonequilibrium Bose condensation in a weakly interacting gas, J. Moscow Phys. Soc. **1**, 373 (1991).

[36] Y. Kagan, B. V. Svistunov, and G. V. Shlyapnikov, Kinetics of Bose condensation in an interacting Bose gas, Sov. Phys. JETP **75**, 387 (1992).

[37] R. H. Kraichnan, Condensate turbulence in a weakly coupled boson gas, Phys. Rev. Lett. **18**, 202 (1967).

[38] S. Nazarenko, *Wave Turbulence* (Springer, 2011).

[39] E. Gliott, C. Piekarski, and N. Cherroret, Coarsening of binary Bose superfluids: An effective theory, Phys. Rev. Res. **7**, 033189 (2025).

[40] J. Berges, G. S. Denicol, M. P. Heller, and T. Preis, Far from equilibrium hydrodynamics of nonthermal fixed points, arXiv preprint 10.48550/arXiv.2504.18754 (2025).

[41] H. Li, X.-H. Yu, M. Nakagawa, and M. Ueda, Ward-Takahashi identity and gauge-Invariant response theory for open quantum systems, arXiv preprint 10.48550/arXiv.2602.13632 (2026).

[42] R. Mittal, T. Zander, J. Lang, and S. Diehl, Fermion quantum criticality far from equilibrium, Phys. Rev. X **16**, 011069 (2026).

[43] L. P. Pitaevskii and S. Stringari, *Bose-Einstein Condensation and Superfluidity*, 2nd ed. (Oxford University Press, 2016).

[44] H. Zhai, *Ultracold Atomic Physics* (Cambridge University Press, 2021).

[45] L. V. Keldysh, Diagram technique for nonequilibrium processes, Sov. Phys. JETP **20**, 1018 (1965).

[46] A. Kamenev, *Field Theory of Non-Equilibrium Systems* (Cambridge University Press, 2011).

[47] L. M. Sieberer, A. Chiocchetta, A. Gambassi, U. C. Täuber, and S. Diehl, Thermodynamic equilibrium as a symmetry of the schwinger-keldysh action, Phys. Rev. B **92**, 134307 (2015).

[48] A. N. Mikheev, J. Berges, and T. Gasenzer, Nonequilibrium quantum fields in the classical statistical approach, Ann. Phys. **405**, 50 (2019).

[49] I. Gnusov, P. Comaron, A. Gianfrate, D. Trypogeorgos, M. H. Szymanska, P. Cazzato, M. D. Giorgi, D. Sanvitto, and D. Ballarini, Dynamical universality in a driven quantum fluid of light, arXiv preprint 10.48550/arXiv.2605.02397 (2026).

[50] S. J. Morris, M. Gazo, S. M. Fischer, H. Zhang, C. J. Ho, N. R. Cooper, C. Eigen, and Z. Hadzibabic, Observation of vinen turbulence during far-from-equilibrium Bose–Einstein condensation in a homogeneous gas, arXiv preprint 10.48550/arXiv.2604.28191 (2026).

[51] P. C. Hohenberg and B. I. Halperin, Theory of dynamic critical phenomena, Rev. Mod. Phys. **49**, 435 (1977).

[52] B. I. Halperin and D. R. Nelson, Theory of two-dimensional melting, Phys. Rev. Lett. **41**, 121 (1978).

[53] D. R. Nelson, *Defects and Geometry in Condensed Matter Physics*, 1st ed. (Cambridge University Press, Cambridge, 2002) Chap. 2.

[54] J. Durnin, M. J. Bhaseen, and B. Doyon, Nonequilibrium dynamics and weakly broken integrability, Phys. Rev. Lett. **127**, 130601 (2021).

[55] K. Fujii and T. Enss, Hydrodynamic attractor in ultracold atoms, Phys. Rev. Lett. **133**, 173402 (2024).

[56] K. G. Wilson and J. Kogut, The renormalization group and the ϵ expansion, Phys. Rep. **12**, 75 (1974).

[57] S. Sab, M. A. Moreno-Armijos, A. D. García-Orozco, G. V. Fernandes, Y. Zhu, A. R. Fritsch, H. Perrin, S. Nazarenko, and V. S. Bagnato, Universal behavior on the relaxation dynamics of far-from-equilibrium quantum fluids, arXiv preprint 10.48550/arXiv.2603.02182 (2026).

[58] S. Lannig, M. Prüfer, Y. Deller, I. Siovitz, J. Dreher, T. Gasenzer, H. Strobel, and M. K. Oberthaler, Observation of two non-thermal fixed points for the same microscopic symmetry, arXiv preprint (2023), arXiv:2306.16497.

[59] N. Kaschewski, A. Pelster, and C. A. R. Sá de Melo, Equal-spin and opposite-spin density-density correlations in the BCS-BEC crossover: Gauge Symmetry, Pauli Exclusion Principle, Wick's Theorem and Experiments, arXiv preprint 10.48550/arXiv.2602.23019 (2026).

[60] D. Forster, D. R. Nelson, and M. J. Stephen, Large-distance and long-time properties of a randomly stirred fluid, Phys. Rev. A **16**, 732 (1977).